

# Polaron and size effects in optical line shapes of molecular aggregates

Ning Lu<sup>a)</sup> and Shaul Mukamel<sup>b)</sup>

*Department of Chemistry, University of Rochester, Rochester, New York 14627*

(Received 10 September 1990; accepted 12 April 1991)

Optical absorption and fluorescence line shapes of molecular aggregates are calculated using a variational method and the dynamical coherent potential approximation (DCPA) which account for strong exciton–phonon coupling. The formation and the quantum size effects of excitonic polarons are studied.

## I. INTRODUCTION

The study of the interaction of an electron or an exciton with lattice vibrations has a long history.<sup>1,2</sup> Self-trapping of an electron (electronic polaron<sup>3–5</sup>) in deformable lattice and of a phonon-dressed exciton<sup>6</sup> (excitonic polaron) has been studied in various classes of materials, including quasi-one-dimensional molecular crystals and conducting polymers. The current understanding of these phenomena have been reviewed in Refs. 7–13. Theoretical modeling of polarons requires a nonperturbative treatment of the interaction between electrons or excitons with optical and acoustic phonons. Over the years, both static and dynamical aspects of the problem have been studied extensively. The static studies involve the ground state wave function and energy of the coupled exciton–phonon system. These studies led to the distinction between large and small polarons.<sup>3,5,6,14–22</sup> Dynamical studies involve electron, exciton, or energy transport, resulting in the concept of phonon-assisted hopping for small polarons<sup>4,23</sup> and Davydov's<sup>9</sup> soliton solution of a cubic nonlinear Schrödinger equation for a quasi-one-dimensional molecular chain. The exciton transport and the soliton dynamics in one-dimensional molecular chains were studied extensively.<sup>24–30</sup> Turkevich and Holstein<sup>31</sup> have studied the excited-state spectrum of the coupled electron–phonon system using the Born–Oppenheimer adiabatic approximation for the molecular vibrational energy levels. The properties of the coupled exciton–phonon system can be probed optically, using absorption and emission spectroscopy. Sumi<sup>32</sup> and Abe<sup>33</sup> have calculated the absorption and emission spectra of excitonic polarons using a self-consistent Green's function technique, the dynamical coherent potential approximation (DCPA).

The main difficulty of the polaron problem is in the region of strong exciton–phonon coupling in which the lattice relaxation energy is comparable with the exciton bandwidth. In this region, the polaron problem cannot be treated perturbatively. Variational techniques are commonly used for calculating the polaron ground state. In a typical coupled exciton–phonon system, the total number of excitons and the total (exciton + phonon) momentum are conserved, as pointed out by Merrifield<sup>15</sup> and Fischer *et al.*<sup>20,21</sup> However, most authors did not utilize the momentum conservation in

the trial wave functions used for the polaron ground state and soliton dynamics. Most studies for the energy states and the optical spectra of excitonic polarons were carried out either for infinite molecular crystals,<sup>20,21</sup> or for very small aggregates, say, dimers<sup>34–36</sup> and trimers.<sup>36,37</sup>

In this paper we study the exciton–phonon interactions in large molecular aggregates, and examine the effects of the aggregates size<sup>38</sup> on their energies and optical spectra. We calculate the energy levels and oscillator strengths for linear molecular aggregates of size  $N$  varying from  $N=2$  to  $N=80$ . Our study is carried out using two methods: a variational method which utilizes the total (exciton + phonon) momentum conservation, and the DCPA.<sup>17,32,33</sup> The conservation of the total momentum implies that all eigenstates of the coupled exciton–phonon system are electronically delocalized. We specialize to the Einstein (i.e., dispersionless) phonon model. We find that the energy of the lowest polaron state increases with the size  $N$  of the molecular aggregates. We also find that the zero-momentum phonon mode is decoupled from the rest of the phonon modes and exciton states. For large polarons this decoupling leads to a Poisson distribution of shift  $\sim S/N$  for both absorption and fluorescence spectra; i.e., the Stokes shift between the absorption and fluorescence spectra is inversely proportional to the size  $N$  of the molecular aggregates. Here  $S$  is the ratio of the lattice relaxation energy to the phonon energy. This result implies that, by reducing the size of a given molecular aggregate, one can observe a larger Stokes shift. For small polarons the Stokes shift is independent of the size  $N$ . The variational and the DCPA calculations are in qualitative agreement.

The organization of the paper is as follows. In Sec. II we demonstrate that the Hilbert space of the one-exciton states of an  $N$ -molecule aggregate can be partitioned into  $N$  subspaces, differing by the total (exciton + phonon) momentum. This decomposition is applied in Sec. III to the Einstein phonon model. We also show in Sec. III the separation of the zero-momentum phonon mode from the rest of the phonon modes and exciton states. In Sec. IV we develop a variational method for calculating the lowest state in each of the  $N$  momentum subspaces. In Sec. V we show how the DCPA can be used to calculate the absorption and emission spectra of molecular aggregates. In Sec. VI we calculate the fluorescence spectrum originating from the lowest one-exciton state by using the variational method and the DCPA. For small aggregates the calculations are also compared with an exact (matrix diagonalization) calculation. Using the  $N$  lowest

<sup>a)</sup> Present address: Program Development Corporation, 300 Hamilton Avenue, Suite 409, White Plains, NY 10601.

<sup>b)</sup> Camille and Henry Dreyfus Teacher/Scholar.

states for the  $N$  momentum subspaces obtained in Sec. IV, we construct in Sec. VII a complete basis set, which approximately diagonalizes the Hamiltonian for one-exciton states. In Sec. VIII we calculate the absorption spectrum for optical transitions between zero- and one-exciton states using the variational method and the DCPA. The calculations are also compared with an exact calculation. Finally, we summarize our results in Sec. IX.

**II. THE EXCITON-PHONON HAMILTONIAN**

We consider a cyclic, one-dimensional aggregate of  $N$  coupled molecules. Each molecule is assumed to have two electronic levels and a single intramolecular vibration. The exciton-phonon interaction is taken to be linear in the phonon coordinate. We adopt the Fröhlich Hamiltonian<sup>2</sup> for the coupled exciton-phonon system,

$$H = H_{\text{ex}} + H_{\text{ph}} + H_{\text{int}}, \tag{2.1a}$$

with

$$H_{\text{ex}} = \sum_{k=0}^{N-1} E(k) a_k^\dagger a_k, \tag{2.1b}$$

$$H_{\text{ph}} = \sum_{q=0}^{N-1} \hbar\omega_q \left( b_q^\dagger b_q + \frac{1}{2} \right), \tag{2.1c}$$

$$H_{\text{int}} = - \sum_{k,q=0}^{N-1} \hbar\omega_q [\lambda(k,q) b_q^\dagger a_{k-q}^\dagger a_k + \text{H.c.}]. \tag{2.1d}$$

Here  $H_{\text{ex}}$  is the Hamiltonian for a single Frenkel exciton band in a perfect rigid chain, and  $a_k$  ( $a_k^\dagger$ ) is the Pauli annihilation (creation) operator of an exciton with momentum  $k$  and energy  $E(k)$ , which satisfy the commutation relation  $a_k a_{k'}^\dagger + a_{k'}^\dagger a_k = \delta_{kk'} + 2a_k a_{k'}^\dagger (1 - \delta_{kk'})$ ;  $H_{\text{ph}}$  is the phonon Hamiltonian,  $b_q$  ( $b_q^\dagger$ ) is the boson annihilation (creation) operator of a phonon with momentum  $q$  and frequency  $\omega_q$ , with the commutation relation  $[b_q, b_{q'}^\dagger] = \delta_{qq'}$ ;  $H_{\text{int}}$  is the phonon-exciton interaction, and H.c. stands for Hermitian conjugate.  $a_k^\dagger$  is related to the Pauli creation operator  $a_n^\dagger$  at site  $n$  by the relation

$$a_k^\dagger = \frac{1}{\sqrt{N}} \sum_{n=1}^N e^{i2\pi kn/N} a_n^\dagger, \quad k = 0, 1, 2, \dots, N-1. \tag{2.2}$$

The eigenstates of  $H_{\text{ph}}$  will be denoted  $|\mathbf{m}\rangle \equiv |m_0, m_1, \dots, m_{N-1}\rangle$  with the eigenvalues  $\sum_{q=0}^{N-1} \hbar\omega_q (m_q + \frac{1}{2})$ , where  $m_q$  is the occupation number of the  $q$ th phonon mode.

The total exciton-number operator commutes with the total Hamiltonian  $H$

$$\left[ \sum_{k=0}^{N-1} a_k^\dagger a_k, H \right] = 0, \tag{2.3}$$

and so does the total momentum operator of the exciton-phonon system

$$\left[ \sum_{k=0}^{N-1} k a_k^\dagger a_k + \hat{P}, H \right] = 0. \tag{2.4}$$

Here

$$\hat{P} \equiv \sum_{q=0}^{N-1} q b_q^\dagger b_q \tag{2.5}$$

is the phonon-momentum operator. Thus the Hamiltonian

$H$  conserves the total number of excitons and the total (exciton + phonon) momentum. We can therefore study the exciton-phonon interaction for a fixed number of excitons and a given total momentum. In this paper we study the optical spectra corresponding to transitions between the zero- and the one-exciton states.

There is only one independent zero-exciton state; the exciton-vacuum state  $|0_{\text{ex}}\rangle$ ,  $a_k |0_{\text{ex}}\rangle = a_n |0_{\text{ex}}\rangle = 0$  for all  $k$  and  $n$  values. Since  $\langle 0_{\text{ex}} | H | 0_{\text{ex}} \rangle = H_{\text{ph}}$ , the zero-exciton Hamiltonian is simply given by

$$H_g = |0_{\text{ex}}\rangle H_{\text{ph}} \langle 0_{\text{ex}}|. \tag{2.6}$$

The eigenstates for  $H_g$  are given by the direct product of the exciton and phonon states, i.e.,  $|0_{\text{ex}}; \mathbf{m}\rangle \equiv |0_{\text{ex}}\rangle |\mathbf{m}\rangle$ . The ground state of  $H_g$ , and consequently that of the entire exciton-phonon system, is  $|0_{\text{ex}}\rangle |0\rangle$  with the zero-point energy  $\frac{1}{2} \sum_{q=0}^{N-1} \omega_q$ , where  $|0\rangle$  is the phonon vacuum state,  $b_q |0\rangle = 0$  for all  $q$ .

There are  $N$  independent one-exciton states. They can be chosen to be either  $N$  localized one-exciton states  $|n\rangle$  ( $n = 1, 2, \dots, N$ ), where  $|n\rangle$  represents the state with a single excitation at site  $n$ , or  $N$  delocalized one-exciton states

$$|k\rangle = \frac{1}{\sqrt{N}} \sum_{n=1}^N e^{i2\pi kn/N} |n\rangle, \quad k = 0, 1, \dots, N-1. \tag{2.7}$$

A delocalized state  $|k\rangle$  has the periodicity of  $N$ ,  $|k\rangle = |k + IN\rangle$  for any integer  $l$ ; we therefore restrict  $k$  in the range of  $0 \leq k \leq N-1$ . Different delocalized states are orthogonal,  $\langle k' | k \rangle = \delta_{k'k}$ . In the delocalized basis, the exciton operators can be written as  $a_k = |0_{\text{ex}}\rangle \langle k|$  and  $a_k^\dagger = |k\rangle \langle 0_{\text{ex}}|$ . Thus the one-exciton Hamiltonian is obtained from Eqs. (2.1) as

$$H_e = \sum_{k=0}^{N-1} E(k) |k\rangle \langle k| + \sum_{q=0}^{N-1} \hbar\omega_q \left( b_q^\dagger b_q + \frac{1}{2} \right) - \sum_{k,q=0}^{N-1} \hbar\omega_q [\lambda(k,q) b_q^\dagger |k-q\rangle \langle k| + \text{H.c.}], \tag{2.8}$$

where we have used the closure relation  $\sum_{k=0}^{N-1} |k\rangle \langle k| = 1$  for the one-exciton states.

The exciton-phonon interaction  $H_{\text{int}}$  couples a state  $|k; \mathbf{m}\rangle \equiv |k; m_0, m_1, m_2, \dots, m_{N-1}\rangle$  to the states  $|k-q; m_0, m_1, m_2, \dots, m_q+1, \dots, m_{N-1}\rangle$  and  $|k+q; m_0, m_1, m_2, \dots, m_q-1, \dots, m_{N-1}\rangle$ . That is to say, when the phonon number in mode  $q$  is increased (decreased) by 1, the exciton momentum  $k$  is decreased (increased) by  $q$ , from  $k$  to  $k-q$  ( $k+q$ ). Starting from a phonon-vacuum state  $|k; 0\rangle$ ,  $H_{\text{int}}$  will couple it only to states which conserve the total (exciton + phonon) momentum, i.e., to the states  $|k - \sum_{q=1}^{N-1} q m_q; \mathbf{m}\rangle$ . We denote  $\bar{k} \equiv k - \sum_{q=1}^{N-1} q m_q$ . All the states  $|k - \sum_{q=1}^{N-1} q m_q; \mathbf{m}\rangle \equiv |\bar{k}; \mathbf{m}\rangle$  therefore form a closed subspace, where  $k$  is the total (exciton + phonon) momentum. There are  $N$  such momentum subspaces,<sup>39</sup> corresponding to  $k = 0, 1, 2, \dots, N-1$ . It should be pointed out that the  $N$  momentum subspaces are complete for the one-exciton states, and any one-exciton state belongs to one of  $N$  subspaces. Moreover, for a given choice of  $\mathbf{m} \equiv \{m_0, m_1, m_2, \dots, m_{N-1}\}$ , there are  $N$  one-exciton states  $|k; \mathbf{m}\rangle$  ( $k = 0, 1, 2, \dots, N-1$ ). No two of them belong to the same

momentum subspace. Consequently, the matrix expression of  $H_e$  is block diagonal with  $N$  blocks. This leads to the decomposition,  $H_e = \sum_{k=0}^{N-1} H_k$ , with the Hamiltonian in the  $k$ th block

$$H_k = E(k - \hat{P}) + \sum_{q=0}^{N-1} \hbar\omega_q \left[ b_q^\dagger b_q + \frac{1}{2} - \lambda(k - \hat{P}, q) b_q^\dagger - \lambda^*(k - \hat{P}, q) b_q \right]. \quad (2.9)$$

Any state within the  $k$ th subspace, including the eigenstates of the Hamiltonian  $H_k$ , is of the form

$$|\Psi^{(k)}\rangle = \sum_{\mathbf{m}} A_{\mathbf{m}}^{(k)} |\tilde{k}; \mathbf{m}\rangle. \quad (2.10)$$

If a state  $|\Psi^{(k)}\rangle$  is an eigenstate of a Hamiltonian  $H_k$ ,  $H_k |\Psi^{(k)}\rangle = E^{(k)} |\Psi^{(k)}\rangle$ , then it is also an eigenstate of one-exciton Hamiltonian  $H_e$  with the same eigenvalue  $E^{(k)}$ . We note that the aggregate eigenstates represent a delocalized excitonic state, since the probability of electronic excitation at site  $n$  is

$$\langle n | \text{Tr}_{\text{phonon}} [ |\Psi^{(k)}\rangle \langle \Psi^{(k)} | ] | n \rangle = \frac{1}{N} \sum_{\mathbf{m}} |A_{\mathbf{m}}^{(k)}|^2 = \frac{1}{N}, \quad n = 1, 2, \dots, N, \quad (2.11)$$

where the second equality in Eq. (2.11) follows from the use of the normalization condition for the state  $|\Psi^{(k)}\rangle$ . Equation (2.11) implies that the distribution of excitons is delocalized. This result is different from the localized electronic states obtained by Holstein for both large and small polarons.

### III. EINSTEIN PHONON MODEL

We now specialize to the Einstein optical phonon model, in which all phonon modes have the same frequency. The total Hamiltonian in the localized basis is

$$H = \hbar\omega_0 \sum_{n=1}^N \left[ \epsilon_0 a_n^\dagger a_n - \frac{1}{2} B (a_{n+1}^\dagger a_n + a_n^\dagger a_{n+1}) + \left( b_n^\dagger b_n + \frac{1}{2} \right) - \lambda (b_n^\dagger + b_n) a_n^\dagger a_n \right], \quad (3.1)$$

where  $\omega_0 \epsilon_0$  is the 0-0 transition frequency of a free monomer, and the exciton-phonon coupling constant  $\lambda$  is real. Making use of Eq. (2.2) and the relations

$$b_n = \frac{1}{\sqrt{N}} \sum_{q=0}^{N-1} e^{i2\pi qn/N} b_q, \quad n = 1, 2, \dots, N, \quad (3.2)$$

we can transform the Hamiltonian  $H$  in Eq. (3.1) into the form of Eqs. (2.1) with

$$E(k) = \hbar\omega_0 [\epsilon_0 - B \cos(2\pi k/N)], \quad (3.3)$$

$$\omega_q = \omega_0, \quad (3.4a)$$

$$\lambda(k, q) = \lambda / \sqrt{N} \equiv \lambda_N. \quad (3.4b)$$

The exciton bandwidth is  $2B\hbar\omega_0$ . The quantities  $\omega_q$  and  $\lambda(k, q)$  do not depend on the momenta  $k$  and  $q$  for the present model.

When the exciton-phonon coupling parameter  $\lambda(k, 0)$  is independent of the exciton momentum  $k$ , the zeroth phonon mode is decoupled from the other phonon modes and exciton states in the one-exciton case, as can be seen from Eqs. (2.8) and (2.9). As this is indeed the case for the Einstein phonons [see Eq. (3.4b)], we can partition  $H_e$  as

$$H_e = H' + H'', \quad (3.5)$$

with

$$H' = \sum_{k=0}^{N-1} E(k) |k\rangle \langle k| + \hbar\omega_0 \sum_{q=1}^{N-1} \left( b_q^\dagger b_q + \frac{1}{2} \right) - \hbar\omega_0 \lambda_N \sum_{q=1}^{N-1} \sum_{k=0}^{N-1} (b_q^\dagger |k-q\rangle \langle k| + \text{H.c.}), \quad (3.6)$$

$$H'' = \hbar\omega_0 \left[ b_0^\dagger b_0 + \frac{1}{2} - \lambda_N (b_0^\dagger + b_0) \right], \quad (3.7)$$

where  $b_0$  stands for  $b_{q=0}$ . Since it is independent of  $b_0$  and  $b_0^\dagger$ ,  $H'$  commutes with  $H''$ ,

$$[H', H''] = 0. \quad (3.8)$$

Similarly, we can partition the  $k$ th subspace Hamiltonian  $H_k$  as

$$H_k = H'_k + H'', \quad (3.9)$$

with

$$H'_k = \hbar\omega_0 \left\{ \epsilon_0 - B \cos[2\pi(k - \hat{P})/N] + \sum_{q=1}^{N-1} \left[ b_q^\dagger b_q + \frac{1}{2} - \lambda_N (b_q^\dagger + b_q) \right] \right\}. \quad (3.10)$$

$H'_k$  differs from  $H_k$  of Eq. (2.9) only by the exclusion of  $q=0$  phonon mode.

The eigenvalues and eigenstates of the Hamiltonian  $H''$  can be found easily by making a canonical transformation<sup>6</sup>

$$B_0 = D_0(\lambda_N) b_0 D_0(-\lambda_N) = b_0 - \lambda_N, \quad (3.11)$$

where

$$D_q(\alpha) \equiv \exp(\alpha b_q^\dagger - \alpha^* b_q) \quad (3.12)$$

is the displacement operator for the  $q$ th phonon mode, which has the properties  $D_q^\dagger(\alpha) = D_q(-\alpha) = D_q^{-1}(\alpha)$ . The displaced phonon operator  $B_0$  and its adjoint  $B_0^\dagger$  are also Boson operators, since they obey the commutation relation

$$[B_0, B_0^\dagger] = [b_0, b_0^\dagger] = 1. \quad (3.13)$$

It follows from Eqs. (3.7) and (3.11) that  $H''$  now takes the form of a simple harmonic oscillator

$$H'' = \hbar\omega_0 (B_0^\dagger B_0 + \frac{1}{2} - S_N), \quad (3.14)$$

where

$$S_N \equiv \lambda_N^2 \equiv S/N, \quad S \equiv \lambda^2. \quad (3.15)$$

$S$  is the lattice relaxation energy (in the units of  $\hbar\omega_0$ ). We denote the number states of the displaced Boson operator  $B_0$  as  $|j\rangle_0$ ,  $B_0^\dagger B_0 |j\rangle_0 = j |j\rangle_0$ . We thus have

$$H'' |j\rangle_0 = \hbar\omega_0 (j + \frac{1}{2} - S_N) |j\rangle_0, \quad j = 0, 1, 2, \dots, \quad (3.16)$$

where  $\hbar\omega_0 (j + \frac{1}{2} - S_N)$  are the eigenvalues and  $|j\rangle_0$  are

the eigenstates. The lowest eigenstate of  $H''$  is the vacuum state  $|0\rangle_0$  of the displaced phonon operator  $B_0$  with the eigenvalue  $\hbar\omega_0(\frac{1}{2} - S_N)$ . All  $|j\rangle_0$  states constitute another set of complete basis for the zeroth phonon mode.

Since the state  $|0\rangle_0$  is an eigenstate of the phonon annihilation operator  $b_0$ ,

$$b_0|0\rangle_0 = (B_0 + \lambda_N)|0\rangle_0 = \lambda_N|0\rangle_0, \quad (3.17)$$

we conclude that the vacuum state  $|0\rangle_0$  of the displaced operator  $B_0$  is a coherent state of the undisplaced phonon operator  $b_0$ ,

$$\begin{aligned} |0\rangle_0 &= |\lambda_N\rangle_0 = D_0(\lambda_N)|0\rangle_0 \\ &= \sum_{m=0}^{\infty} [p_m(S_N)]^{1/2} |m\rangle_0, \end{aligned} \quad (3.18)$$

where

$$p_m(\theta) = e^{-\theta} \frac{\theta^m}{m!}. \quad (3.19)$$

The Poisson distribution  $p_m(\theta)$  peaks at  $m \approx \theta$ . Similar to Eq. (3.18), other phonon number states  $|j\rangle_0$  of the displaced operator  $B_0$  can also be expanded in terms of the phonon number states  $|m\rangle_0$  of the undisplaced operator  $b_0$ . The relation between the displaced and undisplaced number states is given in Appendix A.

If a state  $|\Phi^{(k)}\rangle$  is an eigenstate of  $H'_k$ ,

$$H'_k |\Phi^{(k)}\rangle = \{ \mathcal{E}^{(k)} + \hbar\omega_0 [\epsilon_0 + \frac{1}{2}(N-1)] \} |\Phi^{(k)}\rangle, \quad (3.20)$$

it then follows from Eqs. (3.9), (3.16), and (3.20) that the Hamiltonian  $H_k$  for the  $k$ th subspace has eigenstates  $|\Phi^{(k)}\rangle|j\rangle_0$  with eigenvalues  $E^{(k)} = \mathcal{E}^{(k)} + \hbar\omega_0(\epsilon_0 + \frac{1}{2}N + j - S_N)$ , i.e.,

$$\begin{aligned} H_k |\Phi^{(k)}\rangle|j\rangle_0 &= [ \mathcal{E}^{(k)} + \hbar\omega_0(\epsilon_0 + \frac{1}{2}N + j - S_N) ] |\Phi^{(k)}\rangle|j\rangle_0, \\ j &= 0, 1, 2, \dots \end{aligned} \quad (3.21)$$

It is easy to see that the state  $|\Phi^{(k)}\rangle|j\rangle_0$  is also an eigenstate of the one-exciton Hamiltonian  $H_e$ .

Equation (3.20) may be solved numerically using a finite basis set. Diagonalizing the Hamiltonian  $H'_k$  is considerably easier than diagonalizing the one-exciton Hamiltonian  $H_e$ . The basis size needed for the matrix diagonalization reduces from  $NM^N$  to  $M^{N-1}$  if we take the first  $M$  phonon-number states for each phonon mode  $b_q$ , or to an even smaller basis size if we choose phonon-number states according to the restriction  $\sum_{q=1}^{N-1} m_q \leq l$ . As the size  $N$  of the molecular aggregates increases, the necessary basis size increases dramatically, making it impossible to diagonalize the huge matrix for the Hamiltonian  $H'_k$ . Thus an alternative way must be sought. In the next two sections we outline two techniques. A variational procedure and a self-consistent Green's function procedure based on the dynamical coherent potential approximation (DCPA). We next apply these techniques to calculate the absorption and the fluorescence lineshapes of molecular aggregates.

#### IV. VARIATIONAL METHOD: THE LOWEST STATE OF EACH MOMENTUM SUBSPACE

A possible state of collective excitations is given by a multimode coherent state. We denote  $\{c_{qk}\}$  as the  $N$ -mode coherent state, produced by the action of a set of displacement operators on the phonon vacuum state,

$$\begin{aligned} |\{c_{qk}\}\rangle &= \prod_{q=0}^{N-1} D_q(c_{qk}\lambda_N)|0\rangle \\ &= \sum_{\mathbf{m}=0}^{\infty} \prod_{q=0}^{N-1} [p_{m_q}(c_{qk}^2 S_N)]^{1/2} |\mathbf{m}\rangle. \end{aligned} \quad (4.1)$$

In Eq. (4.1)  $c_{qk}\lambda_N$  and  $c_{qk}$  are, respectively, the total and relative displacements of the  $q$ th phonon mode for the  $k$ th subspace. Equation (4.1) does not have a well defined momentum and therefore does not exploit the full symmetry of the system as shown in Eq. (2.4). To correct this we postulate a variational trial state  $|\Psi_0^{(k)}\rangle$  of the form of Eq. (2.10) with the coefficients

$$A_{\mathbf{m}}^{(k)} = \prod_{q=0}^{N-1} [p_{m_q}(c_{qk}^2 S_N)]^{1/2}. \quad (4.2)$$

Equation (4.2) uses the coherent-state expansion coefficients of Eq. (4.1) to construct a state with a well defined total (exciton + phonon) momentum. Using Eqs. (2.8), (2.9), (3.3), (3.4), and (4.2), we find that the expectation value of the Hamiltonian  $H_e$  with respect to the trial state  $|\Psi_0^{(k)}\rangle$  is

$$\begin{aligned} E_0^{(k)} &= \langle \Psi_0^{(k)} | H_e | \Psi_0^{(k)} \rangle \\ &= \langle \Psi_0^{(k)} | H_k | \Psi_0^{(k)} \rangle \\ &= \hbar\omega_0 \epsilon_0 + \hbar\omega_0 \sum_{q=0}^{N-1} \left[ S_N (|c_{qk}|^2 - c_{qk} - c_{qk}^*) + \frac{1}{2} \right] \\ &\quad - \frac{1}{2} \hbar\omega_0 B \left\{ \exp \left[ i 2\pi k / N \right] \right. \\ &\quad \left. - S_N \sum_{q=1}^{N-1} |c_{qk}|^2 (1 - e^{-i2\pi q/N}) \right\} + \text{c.c.} \end{aligned} \quad (4.3)$$

The energy  $E_0^{(k)}$  in Eq. (4.3) is a function of  $N$  relative displacements  $c_{qk}$ ,  $q = 0, 1, 2, \dots, N-1$ . The values of  $c_{qk}$  which minimize  $E_0^{(k)}$  are determined by the following equations:

$$\frac{\partial E_0^{(k)}}{\partial c_{qk}} = 0, \quad \frac{\partial E_0^{(k)}}{\partial c_{qk}^*} = 0, \quad q = 0, 1, 2, \dots, N-1. \quad (4.4)$$

Since  $S_N$  is real, it follows from Eqs. (4.4) that all relative displacements  $c_{qk}$  are real, and they satisfy a set of  $N$  nonlinear algebraic equations

$$\begin{aligned} \frac{1}{c_{qk}} &= 1 + \frac{1}{2} B \left\{ (1 - e^{-i2\pi q/N}) \exp \left[ i 2\pi k / N \right] \right. \\ &\quad \left. - S_N \sum_{l=1}^{N-1} c_{lk}^2 (1 - e^{-i2\pi l/N}) \right\} + \text{c.c.} \end{aligned} \quad (4.5)$$

Thus for the  $k$ th subspace, we obtain a set of  $N$  equations for  $N$  relative displacements  $c_{0k}, c_{1k}, c_{2k}, \dots, c_{N-1,k}$ . Equations (4.5) need to be solved numerically. Since the factor  $(1 - e^{-i2\pi q/N})$  on the right-hand side of Eq. (4.5) vanishes for  $q = 0$ , we find from Eq. (4.5) that

$$c_{0k} = 1, \quad (4.6)$$

which implies that the zeroth phonon mode is always in a coherent state  $|\lambda_N\rangle_0$ , independent of the values of the parameters  $B$ ,  $S$ , and  $N$ . This reduces both the number of unknown  $c_{qk}$  for each momentum subspace and the number of the coupled equations to  $N - 1$ . The result (4.6) is in agreement with our previous result in Sec. III.

For  $B > 0$  (e.g., in molecular  $J$  aggregates<sup>40-42</sup>), the bottom of the exciton band is at  $k = 0$  in the absence of the exciton-phonon coupling ( $\lambda = 0$ ). In the presence of the exciton-phonon coupling ( $\lambda \neq 0$ ), the lowest state among all  $H_k$  is that of  $H_{k=0}$ .<sup>7</sup> Making use of Eqs. (4.4), we can show that, if  $c_{qk} = \alpha_q$  ( $q = 0, 1, 2, \dots, N - 1$ ) are a set of solutions for a given  $k$  value, then  $c_{N-q, -k} = \alpha_q$  are also a set of solutions for  $-k$ . Namely we have the relations

$$c_{q,k} = c_{N-q, -k}, \quad q = 1, 2, \dots \quad (4.7)$$

Substituting Eqs. (4.7) into Eq. (4.3) we find that the lowest energies for the momentum subspaces  $k$  and  $-k$  are identical,

$$E_0^{(k)} = E_0^{(-k)}. \quad (4.8)$$

Thus the lowest energy  $E_0^{(k)}$ , as a function of  $k$ , is symmetric about  $k = 0$ . This result is in agreement with the fact that the Hamiltonian of the entire exciton-phonon system is invariant with respect to the change  $k \rightarrow -k$ , as can be seen in Eqs. (3.3) and (3.4). As a special case of Eq. (4.7) we have  $[(N - 1)/2]$  relations

$$c_{q,0} = c_{N-q,0}, \quad q = 1, 2, \dots, [(N - 1)/2] \quad (4.9)$$

for the  $k = 0$  momentum subspace. Here  $[(N - 1)/2]$  stands for the integer part of  $(N - 1)/2$ . Note that for any other subspaces, Eqs. (4.4) do not lead to such relations. This is in contrast to the assumptions made by Fischer and co-workers.<sup>20,21</sup>

In the remainder of this section we shall focus on the zero-momentum subspace ( $k = 0$ ), since  $|\Psi_0^{(0)}\rangle$  is the lowest one-exciton state. Substitution of Eqs. (4.9) into Eqs. (4.3) and (4.5) leads to

$$E_0^{(0)} = \hbar\omega_0 \left( \epsilon_0 + \frac{1}{2} N \right) + \hbar\omega_0 S_N \sum_{q=0}^{N-1} (c_{q0}^2 - 2c_{q0}) - \hbar\omega_0 B \exp \left( -2S_N \sum_{q=1}^{N-1} c_{q0}^2 \sin^2 \frac{\pi q}{N} \right), \quad (4.10)$$

$$\frac{1}{c_{q0}} = 1 + 2B \sin^2 \frac{\pi q}{N} \exp \left( -2S_N \sum_{l=1}^{N-1} c_{l0}^2 \sin^2 \frac{\pi l}{N} \right), \quad (4.11)$$

$$q = 1, 2, \dots, [N/2].$$

Thus the number of equations to be solved is reduced from  $N$  to  $\sim N/2$ . It is easy to see that, when  $B > 0$ , the possible values for  $c_{q0}$  are bound between 0 and 1, i.e.,  $0 < c_{q0} < 1$ .

In the infinite aggregate limit ( $N \rightarrow \infty$ ), we treat the relative displacements  $c_{q0}$ 's as a continuous function of phonon momentum  $q$  and thus replace the summation in Eq. (4.11) by an integral. Solving the resulting simple integral equation, we obtain

$$c_{q0} = \frac{1}{1 + 2B\eta \sin^2(\pi q/N)}, \quad q = 0, 1, 2, \dots, \quad (4.12)$$

where  $\eta$  needs to be determined self-consistently from a nonlinear equation

$$\eta = \exp \left[ -\frac{S}{(1 + 2B\eta)^{3/2}} \right]. \quad (4.13)$$

Even without solving Eq. (4.13) numerically, we can determine the range of the parameter  $\eta$ . First, it is easy to see that  $0 < \eta < 1$ . Then, since the right-hand side of Eq. (4.13) increases monotonically for increasing  $\eta$  as illustrated in Fig. 1, we find that

$$\exp(-S) < \eta < \exp \left[ -\frac{S}{(1 + 2B)^{3/2}} \right]. \quad (4.14)$$

The energy of the lowest one-exciton state is found after substituting Eqs. (4.12) into Eq. (4.10),

$$E_0^{(0)} = \hbar\omega_0 \left[ \epsilon_0 + \frac{1}{2} N - S \frac{1 + 3B\eta}{(1 + 2B\eta)^{3/2}} - B\eta \right], \quad (4.15)$$

which tends to the value  $\hbar\omega_0(\epsilon_0 + \frac{1}{2}N - S)$  when  $\eta$  approaches zero. Equation (4.13) may have one solution within the range of Eq. (4.14), which gives the minimum value of the energy  $E_0^{(0)}$ . Equation (4.13) may also have three solutions  $\eta_1 < \eta_2 < \eta_3$  for larger values of  $S$  and  $B$ . In this case, the smallest ( $\eta_1$ ) and the largest ( $\eta_3$ ) solutions lead to two minima of the total energy, whereas the intermediate solution  $\eta_2$  gives a maximum value of the total energy. For sufficiently large  $S$  and  $B$ , we have approximately  $\eta_1 = e^{-S} \ll 1$  and  $\eta_3 = \exp[-S/(1 + 2B)^{3/2}]$ . Corresponding to  $\eta_1$  all

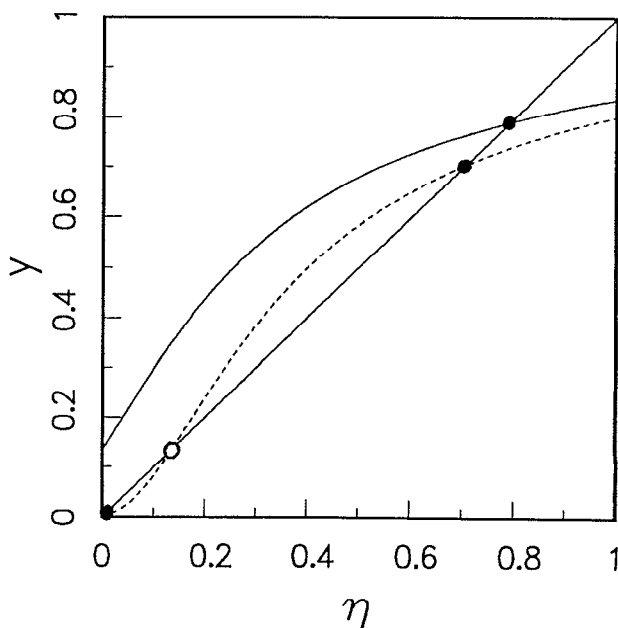


FIG. 1. Graphical solution of Eq. (4.13). The straight line ( $y = \eta$ ) represents the left-hand side of Eq. (4.13), whereas the curves represent the right-hand side. The solid curve is for  $B = 2$  and  $S = 2$ , for which there is one root for Eq. (4.13); The dashed curve is for  $B = 4$  and  $S = 6$ , for which there are three roots for Eq. (4.13). A closed (open) circle represents a minimum (maximum) value of the energy  $E_0^{(0)}$ .

$c_{q0}$  are close to 1, and this situation is usually denoted a small-polaron (localized<sup>20</sup>) state. Note that the state is electronically delocalized and all sites have the same probability ( $1/N$ ) of electronic excitation, as shown in Eq. (2.11). We therefore denote this state a large-phonon-displacement (LPD) state. Corresponding to  $\eta_3$ , most of the  $c_{q0}$  (except a few  $c_{q0}$  with  $q$  close to 0 and to  $N$ ) are  $c_{q0} \ll 1$  when  $B \gg 1$  and  $\eta_3 \sim 1$ . This is usually denoted a large-polaron (delocalized<sup>20</sup>) state. We shall denote it a small-phonon-displacement (SPD) state. Whether we should choose  $\eta_1$  or  $\eta_3$  depends on which one of them gives lower energy  $E_0^{(0)}$  when substituted in Eq. (4.15). We found that, when  $B \gg S$ ,  $\eta_3$  leads to a lower energy than  $\eta_1$  does, and the lowest one-exciton state is an SPD state. When  $B < S$ , the situation is reversed; i.e., the lowest one-exciton state is an LPD state.

For finite-size aggregates, we need to solve Eqs. (4.11) numerically to find the minimum value of  $E_0^{(0)}$  [see Eq. (4.10)]. The situation is similar to that discussed above; namely we may find several sets of solutions for the relative displacements  $c_{q0}$  and we need to choose one set of  $c_{q0}$  which gives the global minimum of  $E_0^{(0)}$ . We plot such a set of  $c_{q0}$  in Fig. 2 for the case of  $B = 10$  and  $S = 10$  with  $N = 2, 3, 10$ , and 40. The resulting values of  $c_{q0}$  show that, for each of  $N$  values, the polaron state is an SPD state (i.e., a large-polaron state), since, except a few  $c_{q0}$  with  $q/N$  close to 0 or to 1, most  $c_{q0}$  are small so that  $c_{q0}^2 \ll 1$ . We note that all  $c_{q0}$ 's for different aggregate sizes, including those for dimer and trimer, fall on a single smooth curve. This implies that the expression (4.12) for large  $N$  gives a very good estimate even for aggregate size as small as  $N = 2$ . We plot Eq. (4.12) for several sets of  $B$  and  $S$  values in Fig. 3, which shows the dramatic difference between an SPD (large-polaron) state

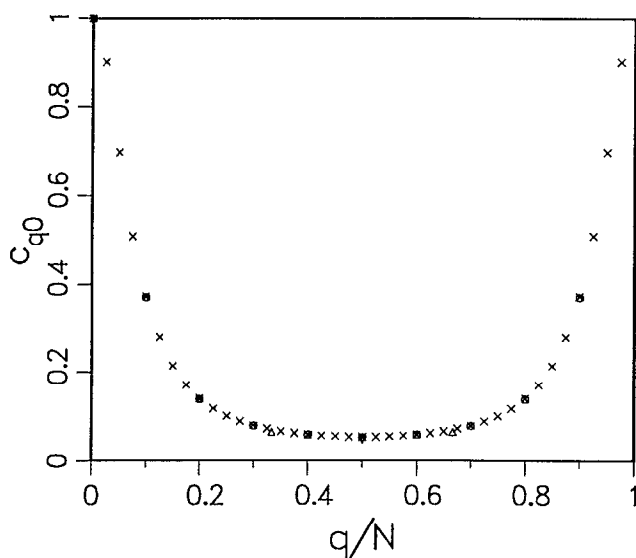


FIG. 2. Relative phonon displacement  $c_{q0}$  vs the phonon momentum  $q$  in the case of  $B = 10$ ,  $S = 10$  for  $N = 40$  ( $\times$ ),  $N = 10$  ( $\circ$ ),  $N = 3$  ( $\Delta$ ), and  $N = 2$  ( $\nabla$ ). Notice the overlap of three symbols  $\times$ ,  $\circ$ , and  $\nabla$  at  $q/N = 0.5$ , and the overlap of  $\circ$  with  $\times$  at other places.

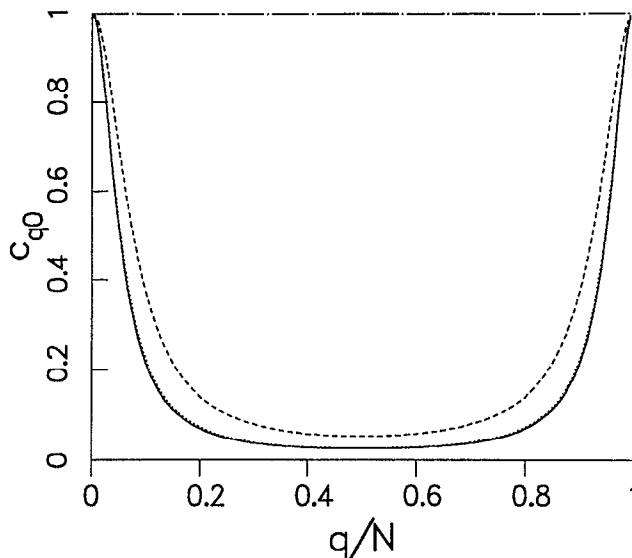


FIG. 3. Relative phonon displacement  $c_{q0}$  vs the phonon momentum  $q$  for an infinite aggregate, as given by Eq. (4.12) for the following sets of parameters:  $B = 20$ ,  $S = 10$  (solid line);  $B = 10$ ,  $S = 10$  (dashed line);  $B = 20$ ,  $S = 20$  (dotted line); and  $B = 5$ ,  $S = 10$  (dash-dot line).

and an LPD (small-polaron) state. For the LPD states, all  $c_{q0} \approx 1$ ; For the SPD states,  $c_{q0}^2 \ll 1$  for most phonon modes except those with  $q/N$  close to 0 or to 1.

In the LPD state with  $B\eta \ll 1$ , we have from Eq. (4.12),  $c_{q0}^2 = 1 - 4B\eta \sin^2(\pi q/N)$ , which is only weakly dependent on the phonon momentum  $q$ . By neglecting the dependence of the relative displacements  $c_{qk}$  on  $q$ , we can obtain, from Eq. (4.3), the effective mass  $m^*$  of the phonon-dressed exciton (polaron) at the bottom ( $k = 0$ ) of the exciton band formed by all  $E_0^{(k)}$ ,

$$m^* = \left( \frac{2\pi\hbar}{N} \right)^2 \left( \frac{d^2 E_0^{(k)}}{dk^2} \right)_{k=0}^{-1} = \frac{\hbar}{\omega_0 B \eta}. \quad (4.16)$$

The effective mass  $m^*$  increases with the lattice relaxation energy  $S$  as  $e^S$  for large enough  $S$  value, since  $\eta = \eta_1 \approx e^{-S}$ . For such a LPD state, we have a very large effective mass for the phonon-dressed exciton, resulting in a very small electron mobility.

Assuming that for a given  $k$  value, all  $c_{qk}$  are identical ( $c_{qk} = C_k$ ), then the energy expression (4.3) reduces to

$$E_0^{(k)} = \hbar\omega_0 \left[ \epsilon_0 + \frac{1}{2}N + S(C_k^2 - 2C_k) - B \cos(2\pi k/N) \exp(-SC_k^2) \right]. \quad (4.17)$$

Equation (4.17) is identical with the expectation value of the energy found by Toyozawa, who postulated a trial state in the localized basis,<sup>19</sup>

$$|\Psi_T^{(k)}\rangle = \frac{1}{\sqrt{N}} \sum_{n=1}^N e^{i2\pi kn/N} |n\rangle D_n(C_k \lambda) |\{0\}\rangle. \quad (4.18)$$

In Eq. (4.18)  $D_n(\alpha)$  is the displacement operator for the localized phonon mode at site  $n$ ,

$$D_n(\alpha) \equiv \exp(\alpha b_n^\dagger - \alpha^* b_n), \quad (4.19)$$

which is analogous to  $D_q(\alpha)$  [see Eq. (3.12)]. Also  $|\{0\}\rangle$  is

the phonon vacuum state in the localized basis,  $b_n|\{0\}\rangle = 0$  for all  $n$ .

Solving Eqs. (3.2) we can express a phonon operator  $b_q$  in the delocalized basis as a linear combination of all phonon operators  $b_n$ 's in the localized basis,

$$b_q = \frac{1}{\sqrt{N}} \sum_{n=1}^N e^{-i2\pi qn/N} b_n, \quad q = 0, 1, 2, \dots, N-1. \quad (4.20)$$

Thus we have  $b_q|\{0\}\rangle = 0$  for any  $q$ . This implies that the localized phonon vacuum state is also the delocalized phonon vacuum state,  $|\{0\}\rangle = |0\rangle$ . It follows from Eqs. (4.19), (3.2), (3.4b), and (3.12) that

$$D_n(C_k \lambda) = \prod_{q=0}^{N-1} D_q(C_k \lambda_N e^{-i2\pi nq/N}). \quad (4.21)$$

Substituting Eq. (4.21) into Eq. (4.18), it is easy to see that the state  $|\Psi_T^{(k)}\rangle$  postulated by Toyozawa is a special case of the state prescribed in Eqs. (2.10) and (4.2) with  $c_{qk} = C_k$  for  $q = 0, 1, 2, \dots, N-1$ .

The optimal choice for the relative displacement  $C_k$  is found by setting  $\partial E_0^{(k)}/\partial C_k = 0$ . This yields the self-consistent equation of Toyozawa,

$$\frac{1}{C_k} = 1 + B \cos(2\pi k/N) \exp(-SC_k^2). \quad (4.22)$$

Similar to determining  $\eta$  in Eq. (4.13), we find that the range of  $C_0$  is

$$\frac{1}{1+B} < C_0 < \frac{1}{1+Be^{-S}}. \quad (4.23)$$

Comparing Eq. (4.22) with Eqs. (4.5), we find that one can obtain Eq. (4.22) alternatively by letting  $c_{qk} = C_k$  in Eqs. (4.5) and summing over  $q$  on both sides of Eqs. (4.5). This shows that the self-consistent equation (4.22) is a special case of Eqs. (4.5). The energy of the lowest one-exciton state is given by  $E_0^{(0)}$ . Two conclusions can now be drawn. First, it is clear that the displacement  $C_0$  determined by Eq. (4.22) is independent of the size  $N$  of the aggregate. Thus Toyozawa's method does not predict any size dependence for the lowest one-exciton state of molecular aggregates. Second, minimizing the energy  $E_0^{(k)}$  in Eq. (4.3) does not lead to equal values of  $c_{qk}$ , as illustrated in Figs. 2 and 3. Consequently, the energy of the lowest one-exciton state given by Toyozawa, determined by Eqs. (4.17) and (4.22), is higher than that given by Eqs. (4.10) and (4.11). Our numerical calculations for  $E_0^{(0)}$  have confirmed this conclusion. Recall that we have  $c_{q0} \approx 1$  for all  $q$  in the case of a LPD state. Thus the trial state proposed by Toyozawa is adequate for the LPD states, but not for the SPD states.

## V. THE DYNAMICAL COHERENT POTENTIAL APPROXIMATION

The optical spectra of molecular aggregates can be calculated by using the DCPA, which is an extension of the static coherent potential approximation (static CPA) for disordered electronic systems. Sumi<sup>17,32</sup> extended the static CPA to calculate the one-particle Green's function<sup>43</sup> in the

DCPA; recently, Abe<sup>33</sup> has extended the DCPA to two-particle Green's function by applying Velicky's<sup>44</sup> formula for the two-particle Green's function in the static CPA. The Green's function technique allows us to calculate directly the experimental observables such as optical lineshapes without calculating the eigenvalues and eigenstates of the system. We review the DCPA in this section.

At zero temperature ( $T=0$ ), the absorption spectrum of the molecular aggregates can be expressed in terms of the Green's function for the one-exciton Hamiltonian  $H_e$  [cf. Eq. (8.1)],

$$I_{ab}(\omega) = 2N \operatorname{Re} \int_0^\infty dt e^{i(\omega + \omega_0 N/2)t} \times \langle k=0;0|e^{-iH_e t/\hbar - \gamma t}|k=0;0\rangle = -2N \operatorname{Im} \langle k=0;0|G_e(z)|k=0;0\rangle, \quad (5.1)$$

where

$$G_e(z) \equiv \frac{1}{z - [H_e/\hbar - (1/2)N\omega_0]} \quad (5.2)$$

is the Green's function for the Hamiltonian  $H_e - \frac{1}{2}N\hbar\omega_0$ ,  $z = \omega + i\gamma$ , and  $\gamma$  is the relaxation rate of the one-exciton states. At any finite temperature ( $T \neq 0$ ), the absorption spectrum cannot be expressed in terms of a single Green's function for the one-exciton Hamiltonian; rather it can only be expressed as an infinite summation of Green's functions involving  $H_e$ .

The DCPA of Sumi replaces the phonon-state averaged Green's function  $\langle 0|G_e(z)|0\rangle$  by an effective Green's function  $G_{\text{eff}}(z)$  which neglects correlated scatterings among different sites (molecules),

$$\langle 0|G_e(z)|0\rangle \approx \frac{1}{z - [H_{\text{eff}}/\hbar - (1/2)N\omega_0]} = \sum_{k=0}^{N-1} \frac{|k\rangle\langle k|}{z - [E(k)/\hbar + v(z)]} \equiv G_{\text{eff}}(z). \quad (5.3)$$

Here

$$H_{\text{eff}} \equiv \sum_{k=0}^{N-1} [E(k) + \hbar v]|k\rangle\langle k| + \frac{1}{2}N\hbar\omega_0 \quad (5.4)$$

is the effective exciton Hamiltonian, and  $v(z)$  is the coherent potential which depends on the (complex) energy  $z$  but not on the exciton momentum  $k$ . The coherent potential  $v$  is chosen in such a way that the multiple scattering at each single molecule vanishes on the average. At zero temperature  $T=0$ ,  $v(z)$  is calculated from the following self-consistent equation:

$$v(z) = \frac{\omega_0^2 S}{F(z - \omega_0)^{-1} - \frac{2\omega_0^2 S}{F(z - 2\omega_0)^{-1} - \frac{3\omega_0^2 S}{\ddots}}}. \quad (5.5)$$

Here

$$F(z)^{-1} = G(z)^{-1} + v(z), \quad (5.6)$$

whereas

$$G(z) \equiv \langle n | G_{\text{eff}}(z) | n \rangle = \frac{1}{N} \sum_{k=0}^{N-1} \frac{1}{z - E(k)/\hbar - v(z)} \quad (5.7)$$

is a diagonal element of the effective Green's function in the localized electronic basis and is independent of the chosen site  $n$ . One sees from Eq. (5.5) that in the DCPA the coherent potential  $v(z)$  should be determined self-consistently with the coherent potentials  $v(z - p\omega_0)$  ( $p = 1, 2, \dots$ ) at lower energies  $z - p\omega_0$ . In actual numerical calculations, we can first set  $v(z) = 0$  for  $\omega \leq [\epsilon_0 - (10S + 5)]\omega_0$ , and then evaluate  $v(z)$  for  $\omega > [\epsilon_0 - (10S + 5)]\omega_0$  (recall that  $z = \omega + i\gamma$ ). Substitution of Eq. (5.3) into Eq. (5.1) gives the absorption spectrum expressed in terms of the coherent potential,

$$I_{\text{ab}}(\omega) = -2N \text{Im} \langle k=0 | G_{\text{eff}}(z) | k=0 \rangle = -2N \text{Im} \frac{1}{z - E(0)/\hbar - v(z)}. \quad (5.8)$$

The energy of the lowest one-exciton state can also be determined by using the DCPA; it is the energy of the absorption peak with the lowest energy.

At zero temperature ( $T = 0$ ), the steady-state fluorescence spectrum may be expressed in terms of a two-particle Green's function for the exciton-phonon system,<sup>45,46</sup>

$$I_{\text{em}}(\omega) = \langle k=0; \mathbf{0} | G_e(z_i^*) \times \frac{\gamma |k=0\rangle \langle k=0|}{\gamma^2 + \{\omega_i - [H_{\text{ph}} - (1/2)N\omega_0] - \omega\}^2} \times G_e(z_i) | k=0; \mathbf{0} \rangle, \quad (5.9a)$$

where  $\omega_i$  is the frequency of the exciting electromagnetic field,  $z_i = \omega_i + i\gamma$ , and  $\omega$  is the emission frequency. The averaged two-particle Green's function (i.e., the average of a product of two Green's functions) can be calculated by using Velicky's method,<sup>44</sup> which is based on neglecting correlations between different sites. The result is

$$I_{\text{em}}(\omega) \approx \sum_{j=0}^{\infty} \frac{\gamma K_j(\omega_i, \omega_i)}{\gamma^2 + (\omega_i - j\omega_0 - \omega)^2}. \quad (5.9b)$$

In Eq. (5.9b)  $K_j$  is the two-particle Green's function,

$$K_j(\omega_1, \omega_2) = g(z_1)g(z_2^*)\delta_{j,0} + \frac{g(z_1 - j\omega_0)}{\sqrt{N}} \frac{g(z_2^* - j\omega_0)}{\sqrt{N}} \times Q_j(z_1, z_2^*) \frac{g(z_1)}{\sqrt{N}} \frac{g(z_2^*)}{\sqrt{N}}, \quad (5.10)$$

where  $g(z) \equiv \langle k=0 | G_{\text{eff}}(z) | k=0 \rangle = [z - E(0)/\hbar - v(z)]^{-1}$ ,  $z_1 = \omega_1 + i\gamma$ ,  $z_2 = \omega_2 + i\gamma$ , the factors  $1/\sqrt{N}$  originate from the overlap  $\langle k=0 | n \rangle$  between the  $|k=0\rangle$  state and the state localized on a single site, and the vertex part  $Q_j$  is given by the  $(j, 0)$  element of a matrix product,

$$Q_j(z_1, z_2^*) = N \{ \tilde{\Lambda}(z_1, z_2^*) \times [1 - \tilde{R}(z_1, z_2^*) \tilde{\Lambda}(z_1, z_2^*)]^{-1} \}_{j,0}. \quad (5.11)$$

Here the  $(j, l)$  elements ( $j, l \geq 0$ ) of matrices  $\tilde{\Lambda}$  and  $\tilde{R}$  are defined as  $\tilde{\Lambda}_{j,l}(z_1, z_2^*) = \Lambda_{j-l}(z_1 - l\omega_0, z_2^* - l\omega_0)$  and  $\tilde{R}_{j,l}(z_1, z_2^*) = \delta_{j,l} R(z_1 - l\omega_0, z_2^* - l\omega_0)$ .  $\Lambda_j(z_1, z_2^*)$  is the averaged product of the two  $t$ -matrix operators on the same site, and is given by

$$\Lambda_j(z_1, z_2^*) \equiv \begin{cases} t_j(z_1; 0)t_j(z_2^*; 0), & j \geq 0 \\ 0, & j < 0. \end{cases} \quad (5.12)$$

Thus the matrix  $\tilde{\Lambda}$  is a lower triangular matrix, and so is  $1 - \tilde{R}\tilde{\Lambda}$ . In Eq. (5.12) the  $t$  matrices are given by

$$t_0(z; 0) = 0, \quad (5.13a)$$

$$t_j(z; 0) = \frac{D_j(z; 0)}{G(z - j\omega_0)G(z)}, \quad j = 1, 2, \dots, \quad (5.13b)$$

with

$$D_0(z; 0) = G(z) \quad (5.14a)$$

$$D_1(z; 0) = [1 - D_0(z; 0)F(z)^{-1}]/\sqrt{S} = -G(z)v(z)/\sqrt{S}, \quad (5.14b)$$

$$D_j(z; 0) = -\frac{D_{j-1}(z; 0)F(z - j\omega_0 + \omega_0)^{-1}}{\sqrt{jS}} - \sqrt{\frac{j-1}{j}} D_{j-2}(z; 0), \quad j = 2, 3, \dots. \quad (5.14c)$$

The quantity  $R(z_1, z_2^*)$  is a restricted propagator,

$$R(z_1, z_2^*) = \frac{G(z_1) - G(z_2^*)}{v(z_1) - z_1 - [v(z_2^*) - z_2^*]} - G(z_1)G(z_2^*). \quad (5.15)$$

The coherent potential has the property  $v(z^*) = v^*(z)$ , which leads to a similar property for several other quantities,  $G_{\text{eff}}(z)$ ,  $G(z)$ ,  $g(z)$ ,  $F(z)$ ,  $D_j(z; 0)$  ( $j = 0, 1, 2, 3, \dots$ ), and  $t_j(z; 0)$  ( $j = 0, 1, 2, \dots$ ). These properties are helpful in calculating the fluorescence spectrum. In the fluorescence calculations presented below, we found it sufficient to take the size of the matrices  $\tilde{\Lambda}$  and  $\tilde{R}$  to be  $\sim 3S$ .

## VI. THE FLUORESCENCE SPECTRUM

The energy and wave function of the lowest one-exciton state, analyzed in Sec. IV, can be probed experimentally by the fluorescence spectrum from the one-exciton to the zero-exciton states. The fluorescence spectrum of a system driven by a weak, monochromatic electromagnetic field is given by<sup>47</sup>

$$I_{\text{em}}(\omega) = 2 \text{Re} \int_0^{\infty} dt e^{i\omega t} \langle \sigma^\dagger(0)\sigma(t) \rangle = 2 \text{Re} \int_0^{\infty} dt e^{i\omega t} \times \text{Tr} [\rho_{\text{eq}} \sigma^\dagger(0) e^{iH_{\text{st}}t/\hbar} \sigma(0) e^{-i(H/\hbar - i\gamma)t}]. \quad (6.1)$$

Here

$$\sigma \equiv \sum_{n=1}^N a_n = \sqrt{N} a_{k=0}, \quad (6.2)$$

where use has been made of Eq. (2.2). Also in Eq. (6.1),  $\rho_{\text{eq}}$  is the steady-state density operator of the system driven by the electromagnetic field, and we have added an imaginary part  $-i\hbar\gamma$  to the one-exciton Hamiltonian  $H_e$  to represent the relaxation of the exciton from the one-exciton states to the zero-exciton states. Using Eqs. (3.5) and (3.8) we have

$$e^{-iH_e t/\hbar} = e^{-iH_e^*/\hbar} e^{-iH^* t/\hbar}. \quad (6.3)$$

At zero temperature ( $T = 0$ ), we have

$$\rho_{\text{eq}} = \xi |\Phi_0^{(0)}\rangle |0\rangle_0 \langle \Phi_0^{(0)}|_0 \langle 0| + (1 - \xi) |0_{\text{ex}}; \mathbf{0}\rangle \langle 0_{\text{ex}}; \mathbf{0}|, \quad (6.4)$$

where  $|\Phi_0^{(0)}\rangle$  is the lowest eigenstate of Hamiltonian  $H'_0$  in the zero-momentum subspace [cf. Eq. (3.20)] and  $\xi \ll 1$ . Note that the fluorescence is determined solely by the population in the upper states of the fluorescence transitions. Using the separation of the  $q = 0$  phonon mode as illustrated by Eq. (6.3), the trace in Eq. (6.1) can be factorized into a product of two factors. The first involves the zeroth phonon mode only,

$$\langle \sigma^\dagger(0)\sigma(t) \rangle_I = \sum_{m_0=0}^{\infty} p_{m_0}(S_N) e^{i(S_N + m_0)\omega_0 t}, \quad (6.5)$$

which shows a red shift of  $S_N\omega_0$ . In the undisplaced phonon-number-state basis, we write the state  $|\Phi_0^{(0)}\rangle$  as

$$|\Phi_0^{(0)}\rangle = \sum_{\mathbf{m}'=0}^{\infty} A_{\mathbf{m}'}^{(0)} |\tilde{0}; \mathbf{m}'\rangle, \quad (6.6)$$

where the prime ' on a boldface letter indicates the exclusion of the  $q = 0$  phonon mode, i.e.,  $\mathbf{m}' \equiv \{m_1, m_2, \dots, m_{N-1}\}$  and

$$I_{\text{em}}(\omega) = 2\xi N \sum_{l=0}^{\infty} \sum_{m_0=0}^{\infty} \frac{\gamma p_{m_0}(S_N)}{\gamma^2 + [\mathcal{E}_0^{(0)}/\hbar + \omega_0(\epsilon_0 - S_N - m_0 - l) - \omega]^2} \sum_{\mathbf{m}'=0}^l |A_{\mathbf{m}'}^{(0)}|^2 \quad (6.10a)$$

$$= 2\xi N \sum_{j=0}^{\infty} \frac{\gamma W_j}{\gamma^2 + [\mathcal{E}_0^{(0)}/\hbar + \omega_0(\epsilon_0 - S_N - j) - \omega]^2}, \quad (6.10b)$$

where the second equality is obtained by letting  $j = m_0 + l$ . The emission spectrum  $I_{\text{em}}(\omega)$  consists of a progression of equally spaced lines with frequencies  $E_0^{(0)}/\hbar - (\frac{1}{2}N + j)\omega_0 = \mathcal{E}_0^{(0)}/\hbar + \omega_0(\epsilon_0 - S_N - j)$  ( $j = 0, 1, 2, \dots$ ) and weights

$$W_j = \sum_{m_0=0}^j p_{m_0}(S_N) \sum_{\mathbf{m}'=0}^{j-m_0} |A_{\mathbf{m}'}^{(0)}|^2. \quad (6.11)$$

In Eqs. (6.10)  $\omega_0(\epsilon_0 - S_N) + \mathcal{E}_0^{(0)}/\hbar$  is the frequency difference between the lowest one-exciton state  $|\Phi_0^{(0)}\rangle |0\rangle_0$  and the ground state  $|0_{\text{ex}}; \mathbf{0}\rangle$  of the whole exciton-phonon system. Because of the selection rules (6.9), there is no contribution from  $l = 1$  term in Eq. (6.10a). We see from Eq. (6.10a) that, for each  $l$  value, the peaks of the fluorescence spectrum constitute a Poisson distribution with a redshift  $(S_N + l)\omega_0$  and a weight  $\sum_{\mathbf{m}'} |A_{\mathbf{m}'}^{(0)}|^2$ . The envelope of the total fluorescence spectrum is the sum of all individual Poisson envelopes, thus the total (red) Stokes shift is larger than

$|\mathbf{m}'\rangle \equiv |m_1, m_2, \dots, m_{N-1}\rangle$ . The second factor which represents the contribution from the rest of the exciton-phonon system is given by

$$\begin{aligned} \langle \sigma^\dagger(0)\sigma(t) \rangle_{\text{II}} &= \sum_{l=0}^{\infty} \exp\{i[\omega_0(l - \epsilon_0) - \mathcal{E}_0^{(0)}/\hbar]t\} \\ &\quad \times \sum_{m_1 + \dots + m_{N-1} = l} | \langle k=0; \mathbf{m}' | \Phi_0^{(0)} \rangle |^2 \\ &= \sum_{l=0}^{\infty} \exp\{i[\omega_0(l - \epsilon_0) - \mathcal{E}_0^{(0)}/\hbar]t\} \\ &\quad \times \sum_{\mathbf{m}'=0}^l |A_{\mathbf{m}'}^{(0)}|^2. \end{aligned} \quad (6.7)$$

Here  $\mathcal{E}_0^{(0)}$  is defined in Eq. (3.20) with  $\mathcal{E}^{(0)} = \mathcal{E}_0^{(0)}$ ; i.e., the energy of the lowest one-exciton state is

$$E_0^{(0)} = \mathcal{E}_0^{(0)} + \hbar\omega_0(\epsilon_0 + \frac{1}{2}N - S_N) \quad (6.8)$$

[cf. Eq. (3.21)]. In addition, the prime ' on the summation symbol indicates two restrictions in performing summation over  $\mathbf{m}'$ ,

$$\sum_{q=1}^{N-1} m_q = l, \quad (6.9a)$$

$$\frac{1}{N} \sum_{q=1}^{N-1} qm_q = \text{integer}. \quad (6.9b)$$

Equation (6.9b) implies that the  $k = 0$  selection rule for optical transitions selects only those components of the lowest one-exciton state  $|\Phi_0^{(0)}\rangle |0\rangle_0$  which are accompanied by the  $|k = 0\rangle$  one-exciton state. Using Eqs. (6.2), (6.5), and (6.7) in Eq. (6.1), we obtain the steady-state fluorescence spectrum

$S_N\omega_0$ . If only the sum for  $l = 0$  gives a larger weight, which is indeed the case for the SPD (large polaron) states, then the fluorescence spectrum has a Poisson profile with a red shift  $S_N\omega_0$ .

As discussed in Sec. IV, the variational method gives the probability amplitude

$$A_{\mathbf{m}'}^{(0)} = \prod_{q=1}^{N-1} [p_{m_q}(c_{q0}^2 S_N)]^{1/2}. \quad (6.12)$$

After substituting Eq. (6.12) into Eq. (6.11), we find an explicit expression for the weight of the  $j$ th emission component,

$$W_j = \sum_{m=0}^j \prod_{q=0}^{N-1} p_{m_q}(c_{q0}^2 S_N). \quad (6.13)$$

In Eq. (6.13) the double prime " implies two restrictions; Eq. (6.9b) and

$$\sum_{q=0}^{N-1} m_q = j. \quad (6.14)$$

Equation (6.14) is somewhat different from Eq. (6.9a). For each  $j$  value, there always exists one set of  $\mathbf{m}$  satisfying the constraints (6.9b) and (6.14),  $m_0 = j$  and  $m_1 = m_2 = \dots = m_{N-1} = 0$ . For the first two emission components  $j = 0$  and  $j = 1$ , they are the only set of  $\mathbf{m}$  satisfying the conditions (6.9b) and (6.14), and consequently the weights of the emission peaks are

$$W_0 = p_0(S_N) |A_0^{(0)}|^2 = \exp\left(-S_N \sum_{q=0}^{N-1} c_{q0}^2\right), \quad (6.15a)$$

$$W_1 = p_1(S_N) |A_1^{(0)}|^2 = S_N W_0. \quad (6.15b)$$

The intensity ratio  $W_1:W_0$  of the first two emission components is simply  $S_N$ . For  $j = 2$  there are additional  $[N/2]$  sets of  $\mathbf{m}$  satisfying Eqs. (6.9b) and (6.14), such as  $m_l = m_{N-l} = 1$  and all other  $m_q = 0$  ( $l = 1, 2, \dots, [(N-1)/2]$ ) as well as, if  $N$  is even,  $m_{N/2} = 2$  and all the rest of  $m_q = 0$ . For both even- and odd- $N$  cases the weight  $W_2$  can be put into a simple form

$$W_2 = \frac{1}{2} W_0 S_N^2 \sum_{q=0}^{N-1} c_{q0}^4. \quad (6.15c)$$

The intensity ratios of the first three peaks, predicted by the variational method, are

$$\begin{aligned} W_0:W_1:W_2 &= 1:S_N: \frac{1}{2} S_N^2 \sum_{q=0}^{N-1} c_{q0}^4 \\ &= 1:S_N:S_N \frac{S(5B^3\eta^3 + 9B^2\eta^2 + 6B\eta + 2)}{4(1 + 2B\eta)^{7/2}}. \end{aligned} \quad (6.16a) \quad (6.16b)$$

Equation (6.16b) is valid in the  $N \rightarrow \infty$  limit, since we have used Eq. (4.12). As the number  $N$  of the molecules in the aggregate increases to infinity, the intensity ratio  $W_1:W_2$  approaches a constant value [given by (6.16b)], whereas the ratio  $W_0:W_1$  increases linearly with  $N$ .

We display in Fig. 4 the fluorescence spectra of dimers ( $N = 2$ ) and trimers ( $N = 3$ ) using the variational method and the DCPA. The results are compared with an exact (matrix diagonalization) calculation. We choose the same four sets of parameters  $B$  and  $S$  as in Fig. 3. For a dimer, the Hamiltonian  $H_k$  appears in the form of a banded, symmetric matrix with only one codiagonal.<sup>34</sup> Thus the matrix diagonalization for the dimer is very simple. We took the size of the matrix to be  $75 \times 75$  for the dimer. For a trimer, by arranging the basis set in order of increasing sum phonon number ( $m_1 + m_2$ ), the matrix expression of  $H_k$  is a banded, symmetric matrix with  $l$  codiagonals if we choose all bases satisfying  $m_1 + m_2 \leq l$ . The size of such a matrix is  $(l+1)(l+2)/2 \times (l+1)(l+2)/2$ . In order to obtain the correct  $j$ th emission component, one has to have  $l > j$  at least. To obtain an accurate fluorescence spectrum, one needs to take  $l > 2S$ . In the small-polaron region in which the Stokes shift is large, it is better to take a larger  $l$  value. For the calculations presented in this paper, we chose  $l = 25$  for  $B = 20$ ,  $S < 10$  [Fig. 4(a)] and for  $B = 10$ ,  $S = 10$  [Fig. 4(b)], and the size of the corresponding matrices was  $351 \times 351$ . For  $B = 20$ ,  $S = 20$  [Fig. 4(c)], we chose  $l = 45$

and diagonalized a banded  $1081 \times 1081$  matrix. For  $B = 5$ ,  $S = 10$  [Fig. 4(d)], we chose  $l = 30$  and solved the eigenvalue problem of a banded  $496 \times 496$  matrix.

Figure 4(a) is for  $B = 20$  and  $S = 10$ , for which the lowest one-exciton state  $|\Phi_0^{(0)}\rangle$  is a SPD (large-polaron) state for both dimer and trimer. The fluorescence spectrum predicted by the variational method is indistinguishable from that predicted by the exact method (the two differ by only  $\sim 1\%$  at  $j = 5$  and  $j = 4$  for the dimer and at  $j = 3$  for the trimer); each of them has the highest emission peaks at both  $j = 5$  and  $j = 4$  components for the dimer and at  $j = 3$  for the trimer. Thus the fluorescence spectra satisfy the Poisson distribution  $p_j(S_N)$ , which peaks at  $j = S_N$  and  $j = S_N - 1$  if  $S_N$  is an integer, or at  $j = [S_N]$  if  $S_N$  is not an integer. The fluorescence spectra given by the DCPA peak at  $j = 2$  for the dimer and at  $j = 1$  for the trimer, and thus have smaller Stokes redshifts compared with the exact; Also, the energies of the lowest one-exciton states given by the DCPA are obviously higher than the exact ones. Figures 4(b) and 4(c) use two sets of equal  $B$  and  $S$ , for which the lowest one-exciton states are SPD states for both the dimer and the trimer. As in Fig. 4(a), the variational method gives better fluorescence spectra than the DCPA. Unlike Fig. 4(a), we notice a small difference between the spectra predicted by the variational method and the exact spectra; for example, in the case of dimer, while the variational method still predicts two equal highest peaks at  $j = S_N$  and  $j = S_N - 1$ , the exact spectrum has a single highest peak at  $j = S_N$ , indicating a small deviation from the Poisson distribution  $p_j(S_N)$ . Figure 4(d) is for  $B = 5$  and  $S = 10$ , for which the lowest one-exciton state for a given aggregate size  $N$  should be a LPD (small-polaron) state. However, in the case of dimer, the variational method incorrectly predicts that the lowest one-exciton state is a SPD state, whose fluorescence spectrum peaks at  $j = S_N = 5$  and  $j = S_N - 1 = 4$ . This is quite different from the exact fluorescence spectrum, which peaks at  $j = 8$ . The SPD (large-polaron) state given by the variational method has a higher energy, but its fluorescence spectrum is closer to the exact one (peaked at  $j = 10$ ) than the SPD state with a lower energy. In the case of trimer, the lowest one-exciton state is a LPD (small-polaron) state as expected, and the fluorescence spectrum peaks at  $j = 10$  and  $j = 9$  (the exact spectrum peaks at  $j = 8$ ). The fluorescence spectra given by the DCPA exhibit the Stokes shift only if we drop the first two emission components at  $j = 0$  and  $j = 1$ . Proceeding from Fig. 4(a) to Fig. 4(d), we note that the energies of the lowest one-exciton states and the fluorescence spectra given by the variational method become less accurate compared with those given by the exact method. This implies that the variational method works better in the large-polaron region.

In Figs. 5–8 we display the variational and DCPA fluorescence spectra for different aggregate sizes (up to  $N = 80$ ). We observe the following features for a given set of parameters  $B$  and  $S$ . (1) As the size  $N$  of the molecular aggregate increases, the energy of the lowest one-exciton state first increases and then reaches a constant value at  $N \approx 20$ ; both the variational method and the DCPA predict this feature. (2) In the large-polaron region (Figs. 5–7) the enve-

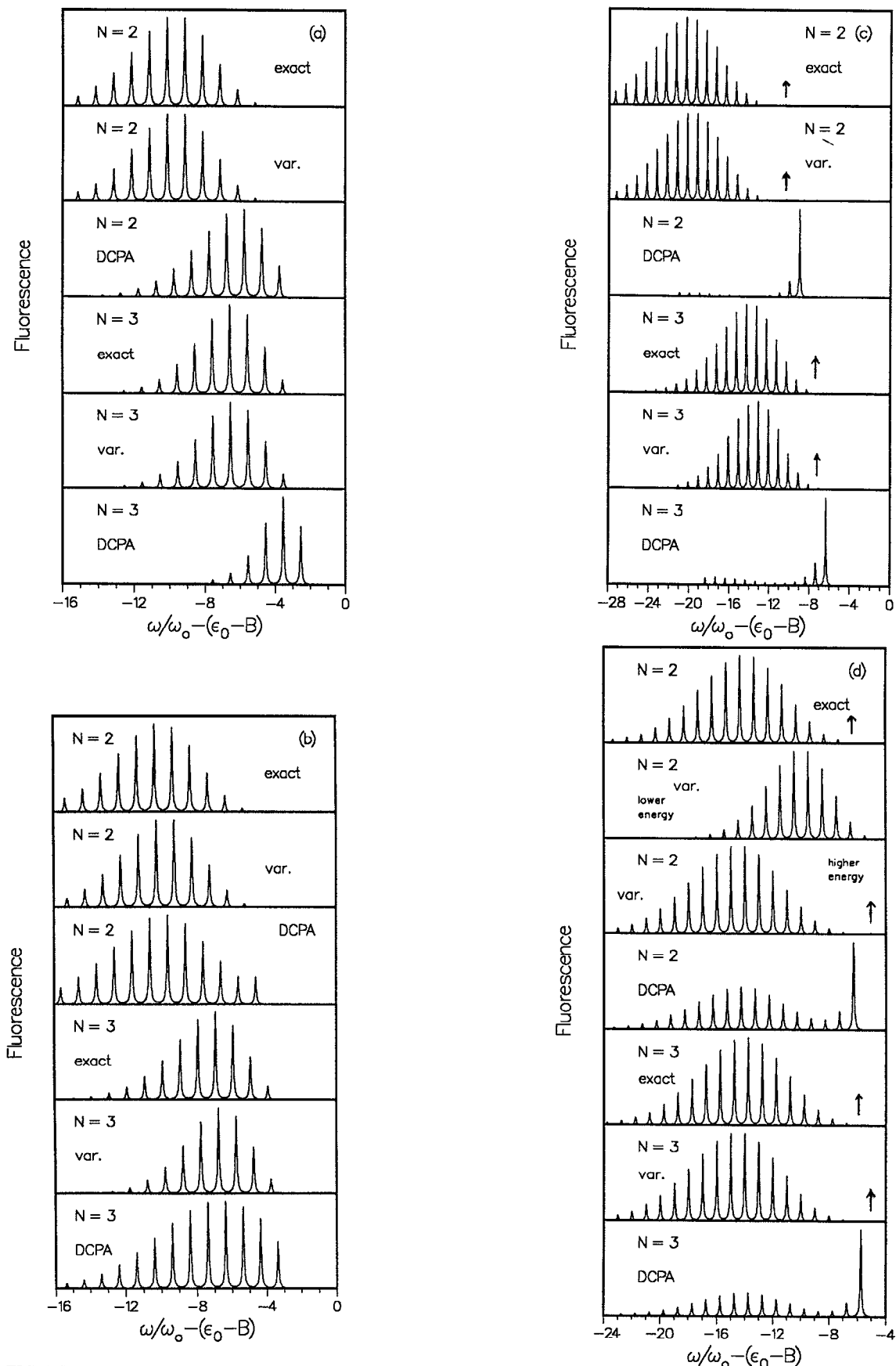


FIG. 4. Steady-state resonance fluorescence spectra of dimers ( $N = 2$ ) and trimers ( $N = 3$ ) for 4 sets of parameters: (a)  $B = 20, S = 10$ ; (b)  $B = 10, S = 10$ ; (c)  $B = 20, S = 20$ ; and (d)  $B = 5, S = 10$ .  $\omega = \omega_0 (\epsilon_0 - B)$  is the transition frequency between the ground state of the exciton-phonon system and the bottom of the exciton band in the absence of exciton-phonon coupling.  $\gamma = 0.05\omega_0$ . When the zeroth phonon emission component is too weak to be seen in the figures, we use an arrow to indicate its position.

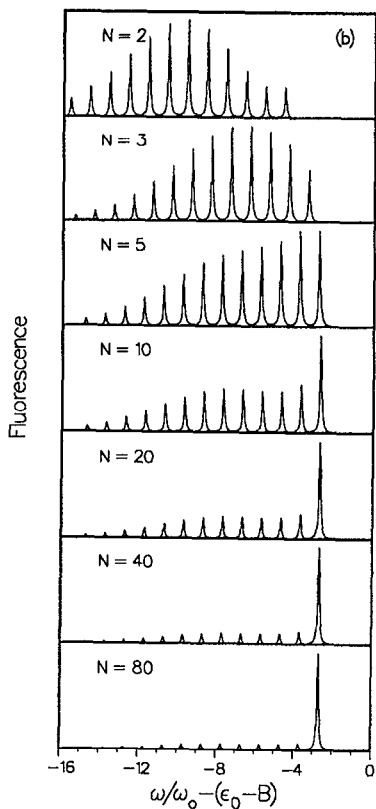
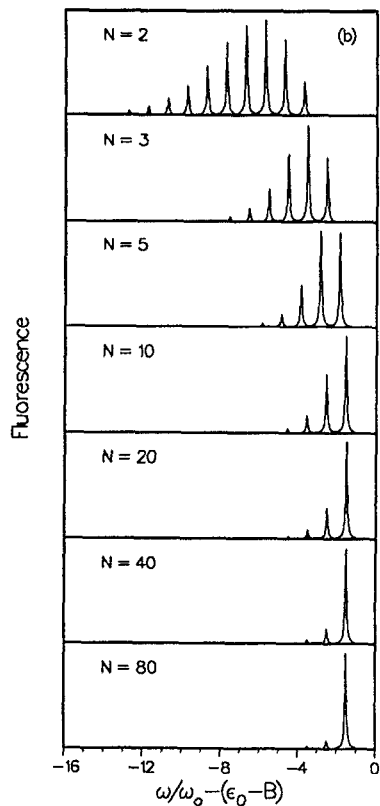
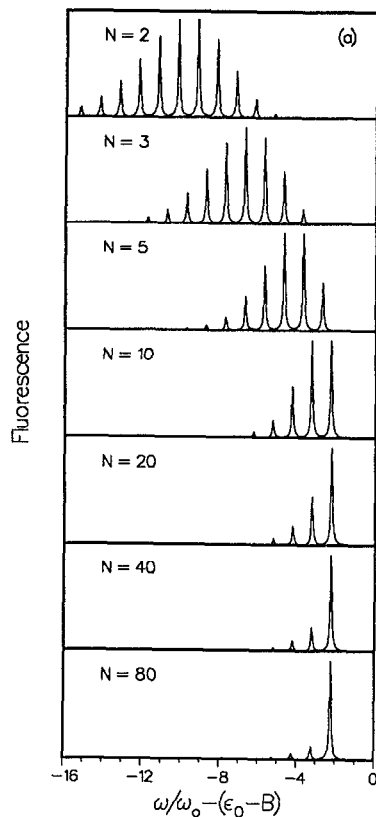
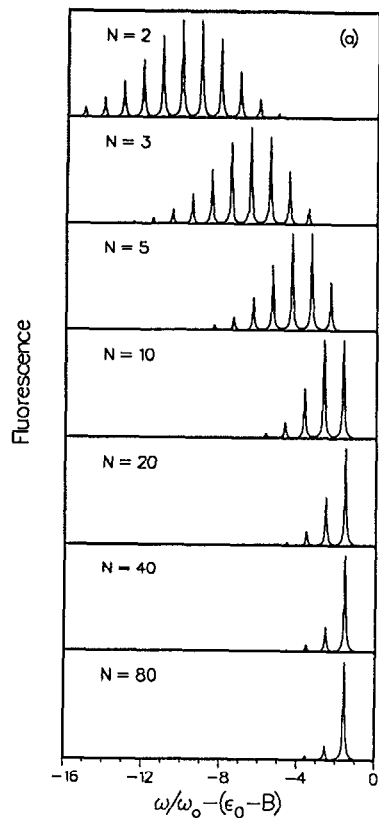


FIG. 5. Steady-state fluorescence spectrum of molecular aggregates of different sizes with  $B = 20$ , and  $S = 10$ . (a) The variational method and (b) the dynamical coherent potential approximation (DCPA).  $\gamma = 0.05\omega_0$ .

FIG. 6. Same as in Fig. 5 but for  $B = 10$  and  $S = 10$ .

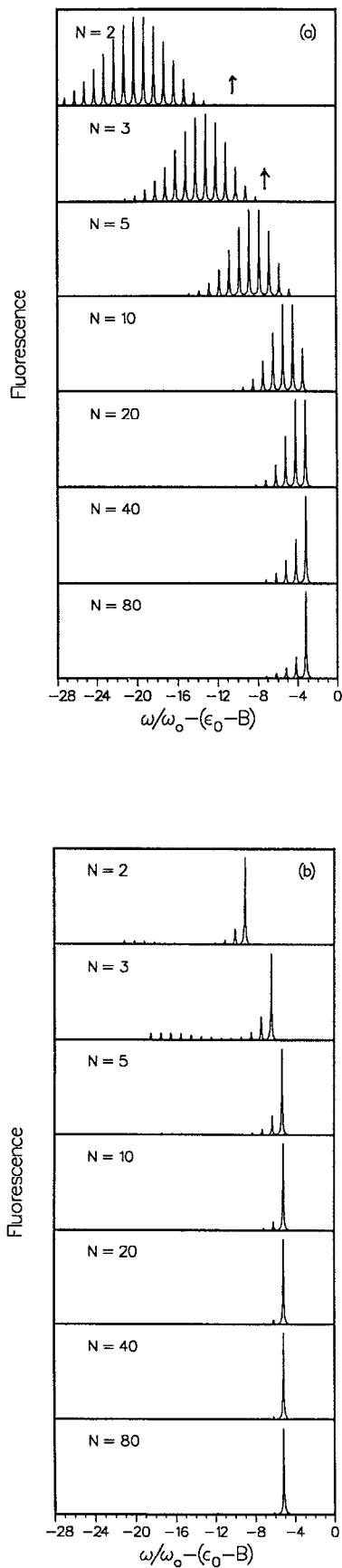


FIG. 7. Same as in Fig. 6 but for  $B = 20$  and  $S = 20$ . When the zeroth phonon emission component is too weak to be seen in the figures, we use an arrow to indicate its position.

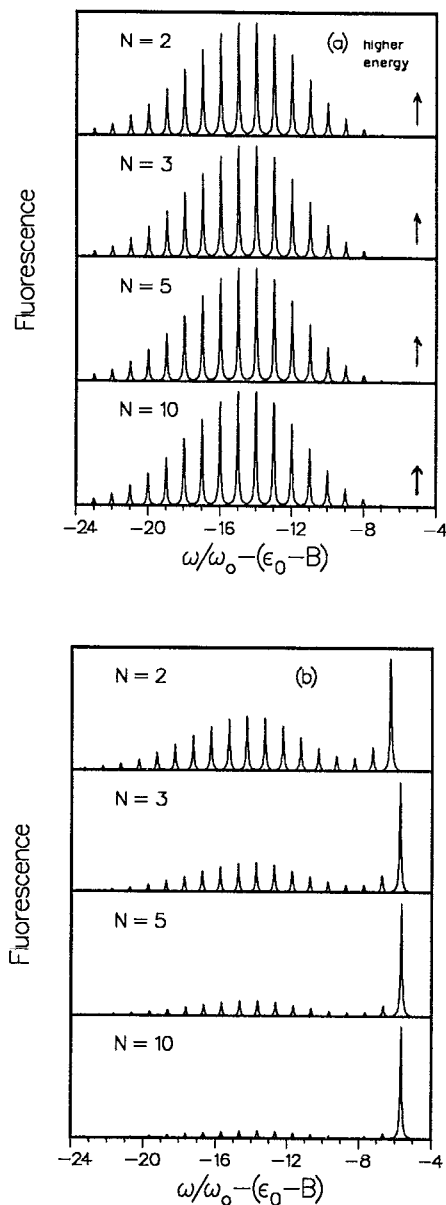


FIG. 8. Same as in Fig. 7 but for  $B = 5$  and  $S = 10$ .

lopes of the fluorescence spectra from both methods show a Stokes shift, which decreases as  $N$  increases; the magnitude of the Stokes shift is approximately  $S_N \omega_0$  from the variational method. When  $N$  exceeds  $S$  (i.e.,  $S_N < 1$ ), the relative intensity ratios of all inelastic emission components (i.e.,  $j = 1, 2, 3, \dots$ ) become constants, whereas the Rayleigh component ( $j = 0$ ) becomes stronger compared with the remaining components. (3) In the small-polaron region (Fig. 8), the envelope of the spectrum also exhibits a redshift; but it is independent of the aggregate size  $N$  (for the DCPA, this can only be seen if we exclude the emission components with  $j = 0$  and  $j = 1$ ).

## VII. THE COMPLETE ONE-EXCITON SPECTRUM

In Sec. IV we formulated a variational method for the lowest eigenstate  $|\Psi_0^{(k)}\rangle$  of the Hamiltonian  $H_k$  for each of

the  $N$  subspaces ( $k = 0, 1, 2, \dots, N - 1$ ). In this section we calculate the complete eigenstates of the Hamiltonian  $H_k$ . These are necessary to calculate the absorption line shapes.

Making use of the phonon displacements  $c_{qk}$  obtained in Sec. IV using the variational method, we now introduce the canonical transformations

$$B_{qk} = D(c_{qk}\lambda_N)b_qD(-c_{qk}\lambda_N) = b_q - c_{qk}\lambda_N, \quad k, q = 0, 1, 2, \dots, N - 1, \quad (7.1)$$

similar to Eq. (3.11). The displaced phonon operators  $B_{qk}$  are also Boson operators, since they satisfy the commutation relation

$$[B_{qk}, B_{qk}^\dagger] = [b_q, b_q^\dagger] = 1. \quad (7.2)$$

Note that the displaced phonon operator  $B_{qk}$  for the  $q$ th phonon mode depends on the total momentum  $k$ , with the exception of the zeroth phonon mode. Since  $c_{0k} = 1$ ,  $B_{0k}$  are simply  $B_0$  introduced in Sec. IV. For each momentum subspace (i.e., for each total momentum  $k$ ), we denote the direct product of the number states of the displaced Boson operators  $B_{qk}$ 's as  $|j\rangle^{(k)}$ ,  $B_{qk}^\dagger B_{qk} |j\rangle^{(k)} = j_q |j\rangle^{(k)}$ ,  $q = 0, 1, \dots, N - 1$ . Similar to the situation of the zeroth phonon mode as discussed in Sec. III [see Eq. (3.18)], the displaced vacuum state  $|0\rangle^{(k)}$  of the operators  $B_{qk}$ 's is simply the coherent state  $|\{c_{qk}\}\rangle$  [see Eq. (4.1)] of the undisplaced operators  $b_q$ 's,  $|0\rangle^{(k)} = |\{c_{qk}\}\rangle$ . Consequently, for each of  $N$  momentum subspaces, the displaced vacuum state  $|0\rangle^{(k)}$  corresponds to the lowest energy state  $|\Psi_0^{(k)}\rangle$  obtained variationally in Sec. IV.

Other energy states of the Hamiltonian  $H_k$  (i.e., in the  $k$ th subspace) can be constructed based on the lowest energy state  $|\Psi_0^{(k)}\rangle$  of  $H_k$ . We take the modified displaced phonon number states

$$|\bar{k}; \mathbf{j}\rangle \equiv \sum_{\mathbf{m}=0}^{\infty} \prod_{q=0}^{N-1} G_{m_q}(j_q, c_{qk}\lambda_N) |\bar{k}; \mathbf{m}\rangle \quad (7.3)$$

as approximate eigenstates of the Hamiltonian  $H_k$ , where

$$G_j(m, \theta) = e^{-\theta/2} \sqrt{j!m!} \sum_{l=0}^{\min(j,m)} \frac{(-1)^{m-l} \theta^{j+m-2l}}{l!(j-l)!(m-l)!}. \quad (7.4)$$

The energy of such a state is found by taking the expectation value of the one-exciton Hamiltonian  $H_e$ ,

$$\begin{aligned} E_{\mathbf{j}}^{(k)} &= \langle \bar{k}; \mathbf{j} | H_e | \bar{k}; \mathbf{j} \rangle \\ &= \langle \bar{k}; \mathbf{j} | H_k | \bar{k}; \mathbf{j} \rangle \\ &= \hbar\omega_0 \sum_{q=0}^{N-1} \left[ j_q + S_N (c_{qk}^2 - 2c_{qk}) + \frac{1}{2} \right] + R_k(\mathbf{j}, \mathbf{j}), \end{aligned} \quad (7.5)$$

which is simply a diagonal matrix element of  $H_k$  on the displaced basis set. The complete expression of  $H_k$  in the displaced basis set is presented in Appendix B. In Eq. (7.5)

$$\begin{aligned} R_k(\mathbf{j}, \mathbf{j}) &= \hbar\omega_0 \epsilon_0 - \frac{1}{2} \hbar\omega_0 B \\ &\times \left[ e^{2\pi k/N} \prod_{q=1}^{N-1} Z(e^{-i2\pi q/N}, j_q, c_{qk}^2 S_N) + \text{c.c.} \right], \end{aligned} \quad (7.6)$$

where

$$\begin{aligned} Z(r, j, u) &= \sum_{m=0}^{\infty} r^m [G_j(m, -\sqrt{u})]^2 \\ &= \frac{e^{u(r-1)}}{j!} \sum_{l,n=0}^j (-1)^{l+n} \binom{j}{l} \\ &\quad \times \binom{j}{n} \sum_{i=0}^{\min(l,n)} \tilde{n} \binom{l}{i} \binom{n}{i} r^{l+n-i} u^{j-i}. \end{aligned} \quad (7.7)$$

Some of the properties of the  $Z$  function is given in Appendix B. When  $\mathbf{j} = \mathbf{0}$ , we recover the wave function and energy of the lowest state of the Hamiltonian  $H_k$ ,

$$|\bar{k}; \mathbf{0}\rangle = |\Psi_0^{(k)}\rangle, \quad (7.8)$$

as can be seen by comparing Eqs. (7.3) and (A4a) with Eqs. (2.10) and (4.2); and

$$E_{\mathbf{0}}^{(k)} = E_0^{(k)}, \quad (7.9)$$

as is evident by contrasting Eqs. (7.5), (7.6), and (B8a) with Eq. (4.3) [ $R_k(\mathbf{0}, \mathbf{0})$  gives exactly the first and last terms of Eq. (4.3)].

When there is only one phonon in the displaced phonon modes so that  $m_q = 1$  and all other  $m_l = 0$  (denoted by  $\{1_q\}$ ), the energy of the state in the  $k = 0$  subspace is approximately

$$\begin{aligned} E_{\{1_q\}}^{(0)} &= \hbar\omega_0 \left( \epsilon_0 + \frac{1}{2} N + 1 \right) + \hbar\omega_0 S_N \sum_{l=0}^{N-1} (c_{l0}^2 - 2c_{l0}) \\ &\quad - \hbar\omega_0 B \exp \left( -2S_N \sum_{l=1}^{N-1} c_{l0}^2 \sin^2 \frac{\pi l}{N} \right) \\ &\quad \times \left[ \cos \frac{2\pi q}{N} + c_{q0}^2 S_N \left( 1 - 2 \cos \frac{2\pi q}{N} + \cos \frac{4\pi q}{N} \right) \right]. \end{aligned} \quad (7.10)$$

Using Eqs. (4.9), it is easy to see that  $E_{\{1_q\}}^{(0)} = E_{\{1_{N-q}\}}^{(0)}$ . When  $q \neq 0$  or  $q \neq N/2$  for even  $N$ , the degeneracy of such states is two, provided  $N \geq 3$ . The function  $f(x) = -\cos x - u(1 - 2 \cos x + \cos 2x)$  has its minimum value  $-1$  at  $x = 0$  if  $u \leq \frac{1}{2}$ , or its minimum value  $1 - 4u$  at  $x = \pi$  if  $u > \frac{1}{2}$ . Since the zeroth phonon mode does not enter into  $R_k(\mathbf{j}, \mathbf{j})$ , we have  $c_{q0}^2 S_N < \frac{1}{2}$  for most SPD states. When  $N$  is large such that  $c_{10}^2 S_N < \frac{1}{2}$  and  $\cos(2\pi/N)$  is close to 1, the second lowest states in the  $k = 0$  subspace are those two states for which  $m_1 = 1$  or  $m_{N-1} = 1$  but all other  $m_l = 0$ . In general, we can show that the energy  $E_{\mathbf{j}}^{(0)}$  for the zero-momentum subspace is invariant under the interchange of all the pairs  $m_q$  and  $m_{N-q}$  ( $q \neq 0$ ). Thus most of the energy levels in the zero-momentum subspace have twofold degeneracy when  $N \geq 3$ . When we solve  $H_k$  exactly by matrix diagonalization as we have done for a trimer ( $N = 3$ ), we find no degeneracy in the zero-momentum subspace. This indicates that the inclusion of the off-diagonal matrix elements of  $H_k$  in the displaced phonon number basis will remove the degeneracy between energies, e.g.,  $E_{\{1_q\}}^{(0)}$  and  $E_{\{1_{N-q}\}}^{(0)}$ .

Equations (7.3) and (7.5) provide a complete basis and corresponding energies, which approximately diagonalize the one-exciton Hamiltonian  $H_e$ . Using this basis set, we can calculate the optical spectra. The steady-state fluorescence spectrum has been studied in Sec. VI. In Sec. VIII we investi-

gate another optical spectrum, the absorption spectrum, which shows the properties of various one-exciton states.

### VIII. ABSORPTION LINE SHAPES

The energies and oscillator strengths of one-exciton states, studied in Sec. VII, can be probed experimentally by the optical absorption from zero-exciton to one-exciton states. The absorption spectrum of a system under the excitation of a weak, cw electromagnetic field is given by<sup>48</sup>

$$\begin{aligned} I_{ab}(\omega) &= 2 \operatorname{Re} \int_0^\infty dt e^{i\omega t} \langle [\sigma(t), \sigma^\dagger(0)] \rangle \\ &= 2 \operatorname{Re} \int_0^\infty dt e^{i\omega t} \operatorname{Tr} [\rho_{\text{eq}} e^{iH_d t/\hbar} \sigma(0) \\ &\quad \times e^{(-iH_d/\hbar - \gamma)t} \sigma^\dagger(0)], \end{aligned} \quad (8.1)$$

where the second equality follows from the assumption that the equilibrium density operator  $\rho_{\text{eq}}$  does not contain any population of one-exciton states. This is certainly true at zero temperature  $T=0$ , at which the equilibrium density operator is simply

$$\rho_{\text{eq}} = |0_{\text{ex}}; \mathbf{0}\rangle \langle 0_{\text{ex}}; \mathbf{0}|. \quad (8.2)$$

Similar to the case of fluorescence spectrum discussed in Sec. VI, the trace in Eq. (8.1) can be factorized into a product of two factors. The first is related to the zeroth phonon mode,

$$\langle \sigma(t) \sigma^\dagger(0) \rangle_{\mathbf{1}} = \sum_{j_0=0}^\infty p_{j_0}(S_N) e^{i(S_N - j_0)\omega_0 t}, \quad (8.3)$$

which now gives a blue shift of  $S_N \omega_0$ . The second results from the rest of the exciton-phonon system,

$$\begin{aligned} \langle \sigma(t) \sigma^\dagger(0) \rangle_{\text{II}} &= \langle \mathbf{0}' | \exp \left[ i\omega_0 t \sum_{q=1}^{N-1} \left( b_q^\dagger b_q + \frac{1}{2} \right) \right] \\ &\quad \times \langle k=0 | e^{-iH_d t/\hbar} | k=0 \rangle | \mathbf{0}' \rangle \\ &= \sum_{\mathbf{j}'=0}^\infty |\langle k=0; \mathbf{0}' | \Phi_{\mathbf{j}'}^{(0)} \rangle|^2 \\ &\quad \times \exp \left[ -i(\omega_0 \epsilon_0 + \mathcal{E}_{\mathbf{j}'}^{(0)}/\hbar) t \right]. \end{aligned} \quad (8.4)$$

Here the last equality is obtained by inserting the closure relation for the Hamiltonian  $H'_k$ , and  $|\Phi_{\mathbf{j}'}^{(0)}\rangle$  is an eigenstate of  $H'_k$  with the eigenvalue  $\mathcal{E}_{\mathbf{j}'}^{(0)} + \hbar\omega_0 [\epsilon_0 + \frac{1}{2}(N-1)]$  [cf. Eq. (3.20)]. We see that the  $k=0$  selection rule selects only the eigenstates of the zero-momentum subspace for the absorption spectrum at zero temperature. Substituting Eqs. (8.3) and (8.4) into Eq. (8.1), we arrive at the explicit expression for the absorption spectrum

$$\begin{aligned} I_{ab}(\omega) &= 2N \sum_{\mathbf{j}'=0}^\infty |\langle k=0; \mathbf{0}' | \Phi_{\mathbf{j}'}^{(0)} \rangle|^2 \\ &\quad \times \sum_{j_0=0}^\infty \frac{\gamma p_{j_0}(S_N)}{\gamma^2 + [\mathcal{E}_{\mathbf{j}'}^{(0)}/\hbar + \omega_0(\epsilon_0 - S_N + j_0) - \omega]^2}. \end{aligned} \quad (8.5)$$

For a given set of  $\mathbf{j}'$ , the contribution from the zeroth phonon mode gives a Poisson distribution with a blueshift  $S_N \omega_0$ . If only one state has a large overlap with the undisplaced phonon vacuum state  $|k=0; \mathbf{0}'\rangle$ , which is indeed the

case for the SPD (large-polaron) states, then the absorption spectrum consists mainly of a single set of equally spaced peaks which form a blueshifted Poisson distribution.

Recall that we have obtained in Eq. (7.3) the eigenfunctions of the one-exciton Hamiltonian  $H_c$  by using the variational method. By noting that  $|\tilde{k}; \mathbf{m}\rangle = |\tilde{k}; \mathbf{m}'\rangle |m_0\rangle_0$  and  $\langle k=0; \mathbf{0}' | = \langle \tilde{0}; \mathbf{0}' |$ , we obtain by using Eqs. (7.3) and (A4b)

$$\langle k=0; \mathbf{0}' | \Phi_{\mathbf{j}'}^{(0)} \rangle = \prod_{q=1}^{N-1} (-1)^{j_q} [p_{j_q}(c_{q0}^2 S_N)]^{1/2}. \quad (8.6)$$

The absorption spectrum predicted by the variational method is obtained after substituting Eq. (8.6) into Eq. (8.5),

$$I_{ab}(\omega) = 2N \sum_{\mathbf{j}'=0}^\infty \frac{\gamma W_{\mathbf{j}'}}{\gamma^2 + [E_{\mathbf{j}'}^{(0)}/\hbar - (1/2)N\omega_0 - \omega]^2}, \quad (8.7)$$

where

$$W_{\mathbf{j}'} = \prod_{q=0}^{N-1} p_{j_q}(c_{q0}^2 S_N) \quad (8.8)$$

is the oscillator strength and  $E_{\mathbf{j}'}^{(0)}$  is the energy given in Eq. (7.5). Note that the summation in Eq. (8.8) is an  $N$ -fold summation, since  $\mathbf{j}' \equiv \{j_0, j_1, \dots, j_{N-1}\}$ . The oscillator strength  $W_0$  of the lowest one-exciton state  $|\Psi_0^{(0)}\rangle$ , which is in the phonon vacuum state of the displaced phonon modes, is equal to  $W_0$  in Eq. (6.15a),  $W_0 = W_0$ . The oscillator strength of a one-phonon state which has the energy  $E_{\{1,q\}}^{(0)}$  [see Eq. (7.10)] is  $c_{q0}^2 S_N W_0$ . For a two-phonon state (in the displaced phonon modes), the oscillator strength is  $c_{q_0}^2 c_{q'_0}^2 S_N^2 W_0$  when one phonon is in the  $q$ th mode and the other in the  $q'$ th mode, and is  $\frac{1}{2} c_{q_0}^4 S_N^2 W_0$  when both phonons are in the same ( $q$ th) phonon mode.

In Fig. 9 we display the absorption spectra of dimer ( $N=2$ ) and trimer ( $N=3$ ) using the variational method and the DCPA. We compare these results with the results of the exact matrix diagonalization. The actual matrix diagonalization for calculating the absorption spectrum is the same as that for calculating the fluorescence spectrum: i.e., we choose the same basis set as for the fluorescence spectrum. We use the same four sets of parameters  $B$  and  $S$  as in Fig. 4 for the fluorescence spectrum. Absorption spectrum also gives the information about the energy of the lowest one-exciton state, which we have described in Sec. VI. Figure 9(a) is plotted for  $B=20$  and  $S=10$ , for which the lowest one-exciton state  $|\Psi_0^{(0)}\rangle$  is a SPD (large-polaron) state for both dimer and trimer. The absorption spectrum predicted by the variational method is very close to the exact; each of them has the highest emission peaks at both  $j_0=5$  and  $j_0=4$  in the case of dimer and at  $j_0=3$  in the case of trimer [see Eq. (8.5)]. Consequently, the absorption spectra also obey the Poisson distribution  $p_{j_0}(S_N)$ , which peaks at  $j_0=S_N$  and  $j_0=S_N-1$  if  $S_N$  is an integer, or at  $j_0=[S_N]$  if  $S_N$  is not an integer. However, the absorption spectra given by the DCPA are quite different from the exact. Figures 9(b) and 9(c) are for  $B=S=10$  and  $B=S=20$ , respectively, for each of which the lowest one-exciton states are SPD states for both the dimer and trimer. As in Fig. 9(a), the variational method gives better absorption spectra than the DCPA, as can be seen by comparing with the exact ab-

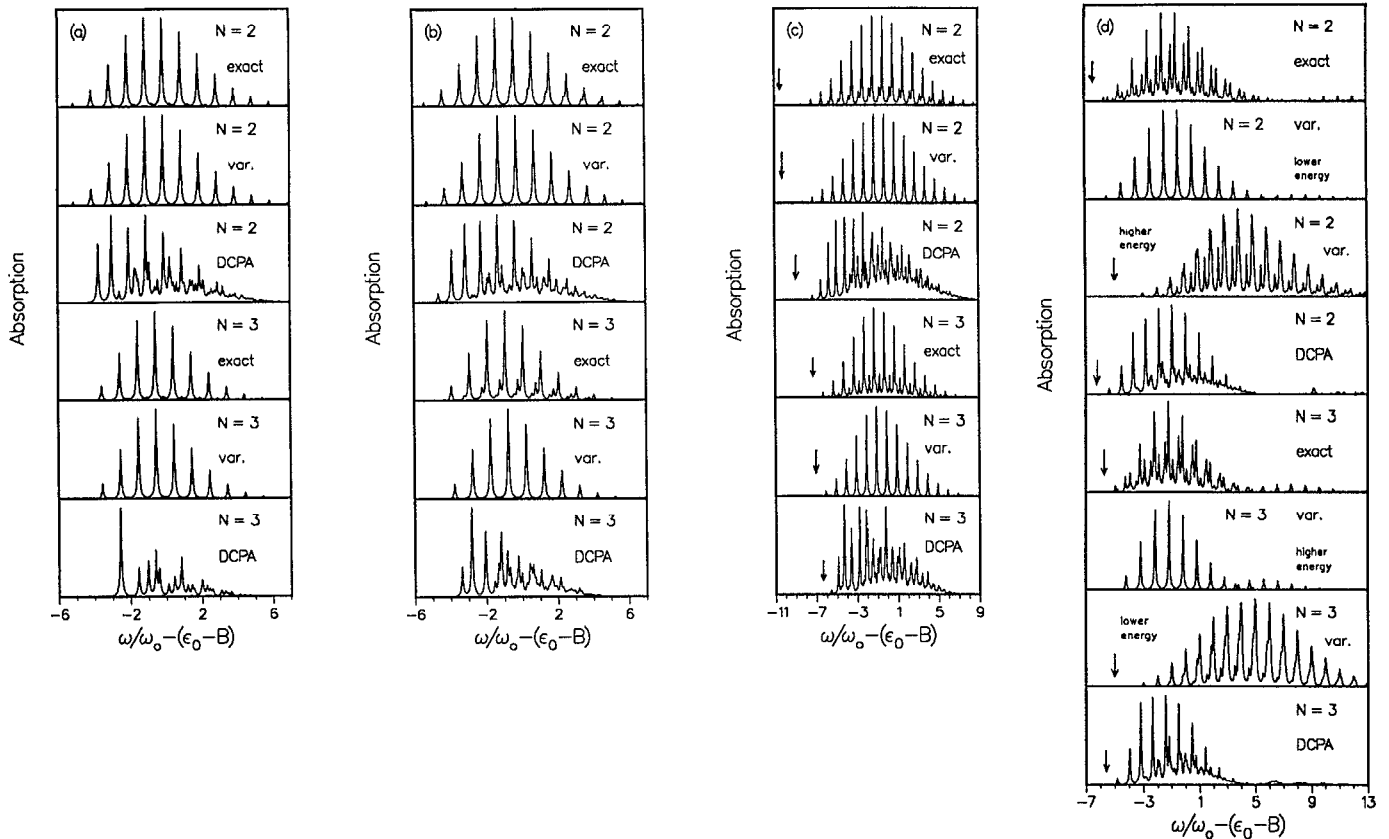


FIG. 9. The absorption spectra of dimers ( $N = 2$ ) and trimers ( $N = 3$ ) for four sets of parameters: (a)  $B = 20, S = 10$ ; (b)  $B = 10, S = 10$ ; (c)  $B = 20, S = 20$ ; and (d)  $B = 5, S = 10$ .  $\gamma = 0.05\omega_0$ . When the absorption peak for the lowest one-exciton state is too weak to be seen, we use an arrow to indicate its position.

sorption spectra. Figure 9(d) is for  $B = 5$  and  $S = 10$ . In the case of dimer, it seems that both the energy and the absorption spectrum suggest that it is in a SPD state. In the case of trimer, the lowest one-exciton state is an LPD (small-polaron) state as expected, but it leads to a less satisfactory absorption spectrum than a SPD state with a higher energy. This means that the variational method is not very accurate for the absorption spectrum in the small-polaron region. Comparing Figs. 9 with Figs. 4, we see that the variational method is more adequate for the fluorescence spectrum than for the absorption spectrum.

In Figs. 10–13 we display the variational and DCPA absorption spectra for different aggregate sizes (up to  $N = 80$ ). We observe the following features for a fixed set of parameters  $B$  and  $S$ . (1) In the large-polaron region (Figs. 10–12) the envelopes of the absorption spectrum from both methods show a blueshift, which decreases as  $N$  increases; The amount of the blueshift is approximately  $S_N\omega_0$  from the variational method. (2) The oscillator strength of the one-exciton states shifts towards the lowest one-exciton state (zero-displaced-phonon state) as the size  $N$  increases. Those states with one or two displaced phonons carry the rest of the oscillator strength of the system.

## IX. CONCLUSIONS

In this paper we have studied the exciton–phonon interaction in one-dimensional, cyclic molecular aggregates and

its manifestation in optical spectra. We found that the Hilbert space of the one-exciton states of an  $N$ -molecule aggregate can be decomposed into  $N$  subspaces. The eigenstates of the one-exciton Hamiltonian  $H_e$  are always delocalized with respect to the electronic excitation. This is different from the lowest one-exciton state obtained by Holstein. In the case of the nearest-neighboring exciton coupling and the Einstein phonons, the zero-momentum phonon mode is decoupled from the rest of phonon modes and exciton states. This gives rise to a Stokes shift  $\omega_0 S/N$ , where  $\omega_0 S$  is the lattice relaxation energy. Assuming that each phonon mode is in a coherent state, we find the lowest state in each of  $N$  momentum subspaces variationally and construct a set of orthonormal basis which approximately diagonalizes the Hamiltonian  $H_e$  for the one-exciton case. We find that the energy of the lowest one-exciton state increases with the size  $N$  of the molecular aggregates. The coherent-state assumption for the phonon modes works very well for the SPD (large-polaron) states but less so for the LPD (small-polaron) states. The lowest one-exciton state postulated by Toyozawa is a special case of our trial state, and has a higher energy than our trial state. We calculated the absorption and emission spectra of molecular aggregates and find an  $S/N$  rule of the Stokes shifts for both absorption and emission spectra in the case of large polaron. For the dimer and the trimer, we also calculated the emission and absorption spectra using exact matrix diagonalization. We find that the fluorescence and absorp-

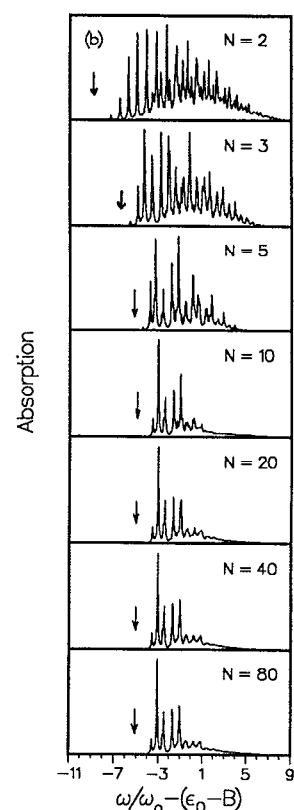
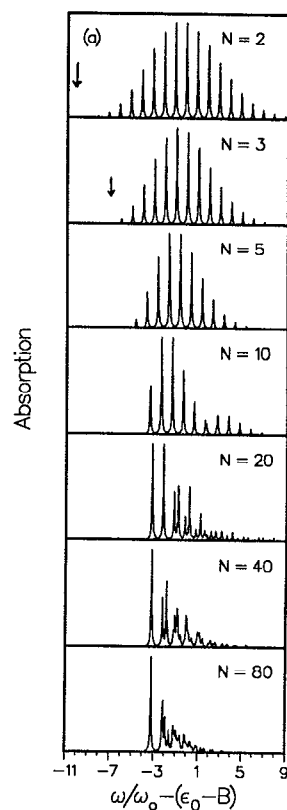
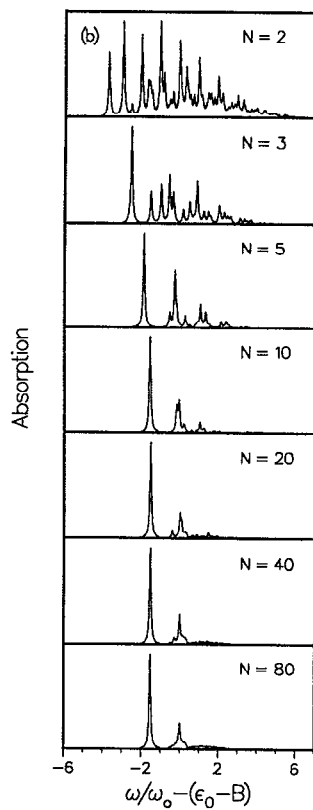
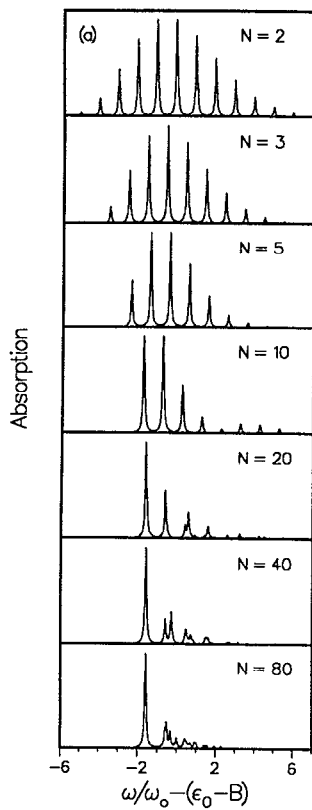


FIG. 10. Absorption spectrum of molecular aggregates of different sizes with  $B = 20$  and  $S = 10$ . (a) The variational method and (b) the DCPA.  $\gamma = 0.05\omega_0$ .

FIG. 12. Same as in Fig. 11 but for parameters  $B = 20$  and  $S = 20$ . When the absorption peak for the lowest one-exciton state is too weak to be seen, we use an arrow to indicate its position.

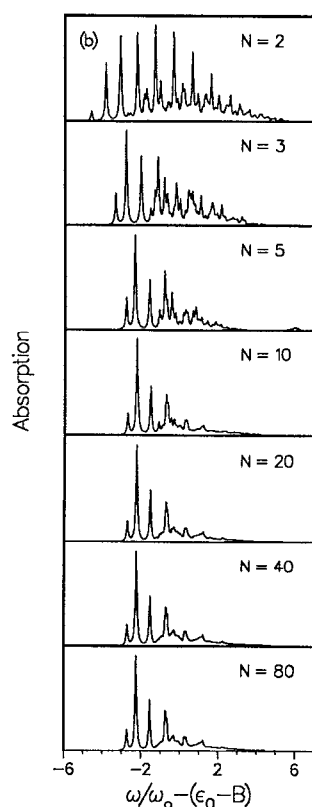
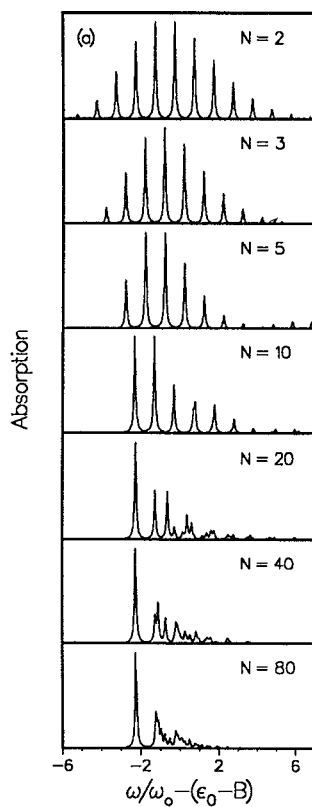


FIG. 11. Same as in Fig. 10 but for parameters  $B = 10$  and  $S = 10$ .

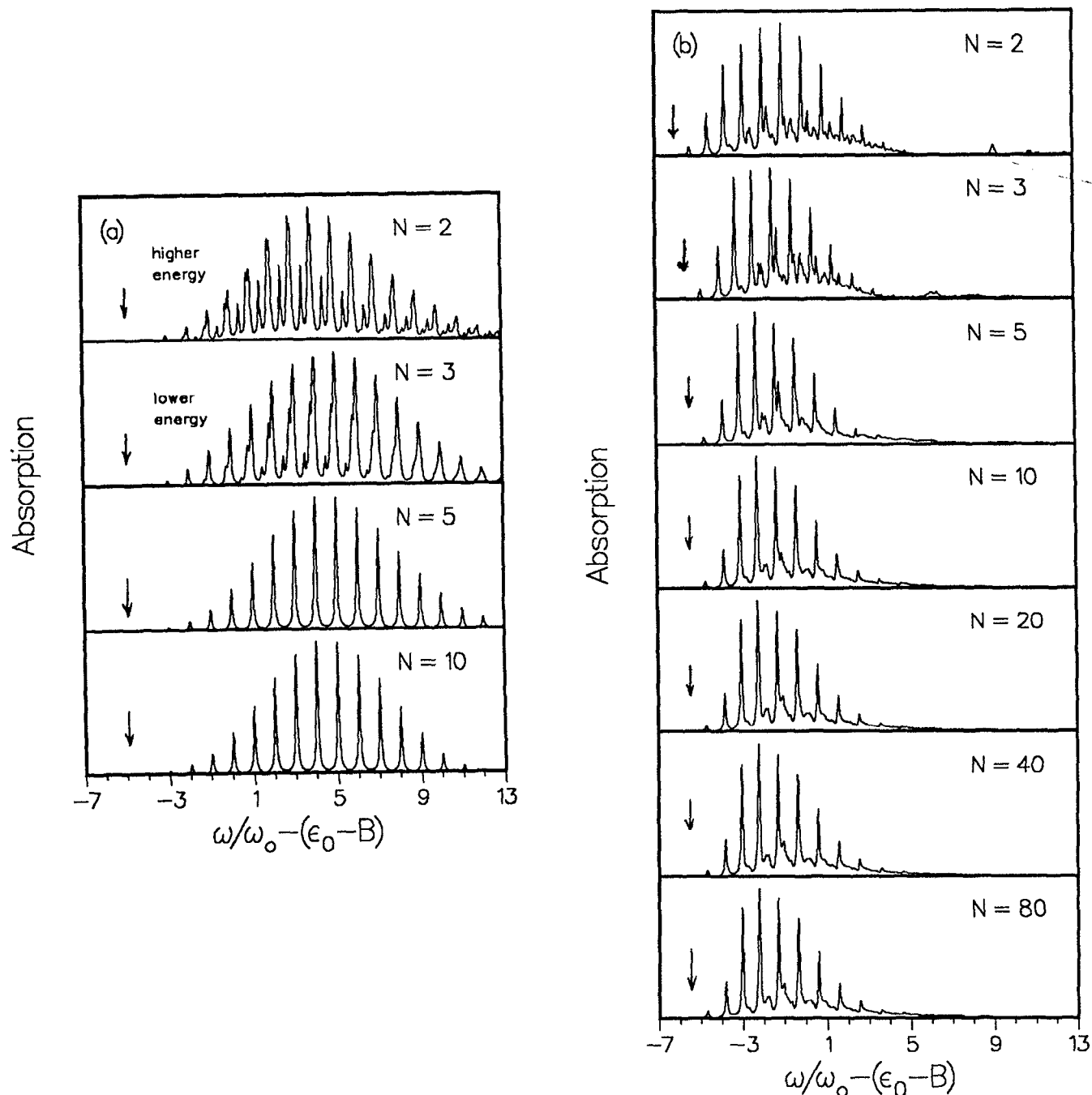


FIG. 13. Similar to Fig. 12 but for parameters  $B = 5$  and  $S = 10$ .

tion spectra using exact matrix diagonalization. We find that the fluorescence and absorption spectra obtained variationally are in good agreement with those obtained exactly in the region of  $S \leq B$  (i.e., in the large-polaron region). We also calculated the fluorescence and absorption spectra of the aggregates by using the DCPA, and found that it reproduces the qualitative features of the spectrum but is less accurate than the variational method for large polarons.

#### ACKNOWLEDGMENTS

We wish to thank S. Abe for discussions concerning the dynamical coherent potential approximation. The support

of the National Science Foundation, the Air Force of Scientific Research, and the Petroleum Research Fund sponsored by the American Chemical Society is gratefully acknowledged.

#### APPENDIX A: THE DISPLACED PHONON NUMBER STATES

The displaced phonon number state  $|j\rangle_0$  is related to the displaced vacuum state  $|0\rangle_0$  by the relation

$$|j\rangle_0 = \frac{1}{\sqrt{j!}} (B_0^\dagger)^j |0\rangle_0. \quad (\text{A1})$$

Similar to Eq. (3.18), we can expand each displaced number state  $|j\rangle_0$  of  $B_0$  in terms of undisplaced number states  $|m\rangle_0$  of  $b_0$  by substituting Eqs. (3.11) and (3.18) into Eq. (A1). After some straightforward algebra, we obtain

$$|j\rangle_0 = \sum_{m=0}^{\infty} G_m(j, \lambda_N) |m\rangle_0, \quad (\text{A2})$$

where

$$\begin{aligned} G_m(j, \theta) &= e^{-\theta^2/2} \sqrt{m!j!} \sum_{l=0}^{\min(j,m)} \frac{(-1)^{j-l} \theta^{m+j-2l}}{l!(m-l)!(j-l)!} \\ &= G_j(m, -\theta) \\ &= (-1)^{m+j} G_m(j, -\theta). \end{aligned} \quad (\text{A3})$$

Some of special  $G_m$ 's are related to the Poisson distribution  $p_m$ ,

$$G_m(0, \theta) = [p_m(\theta^2)]^{1/2}, \quad (\text{A4a})$$

$$G_0(j, \theta) = (-1)^j [p_j(\theta^2)]^{1/2}. \quad (\text{A4b})$$

On the other hand, we can also expand each undisplaced phonon number state  $|m\rangle_0$  in terms of the displaced phonon number states  $|j\rangle_0$ ,

$$|m\rangle_0 = \sum_{j=0}^{\infty} G_j(m, -\lambda_N) |j\rangle_0. \quad (\text{A5})$$

Substituting Eq. (A2) into Eq. (A5) and using Eqs. (A3), we find that the  $G$  functions have the orthonormal properties

$$\sum_{j=0}^{\infty} G_m(j, \theta) G_n(j, \theta) = \sum_{j=0}^{\infty} G_j(m, \theta) G_j(n, \theta) = \delta_{mn}. \quad (\text{A6})$$

## APPENDIX B: THE EXPRESSION OF $H_k$ IN THE DISPLACED BASIS

The Hamiltonian  $H_k$  of Eq. (3.9) can be rewritten in the displaced basis set. Replacing  $b_q$  by  $B_{qk}$  [using Eq. (7.1)] and expanding the undisplaced phonon number states  $|m\rangle$  in terms of the displaced phonon number states  $|j\rangle^{(k)}$  [using Eq. (A5)], we obtain

$$\begin{aligned} H_k &= \hbar\omega_0 \sum_{q=0}^{N-1} \left[ B_{qk}^\dagger B_{qk} - \lambda_N (1 - c_{qk}) (B_{qk}^\dagger + B_{qk}) \right. \\ &\quad \left. + S_N (c_{qk}^2 - 2c_{qk}) + \frac{1}{2} \right] \\ &\quad + \sum_{j,l=0}^{\infty} |\tilde{k}; j\rangle R_k(j, l) \langle \tilde{k}; l|, \end{aligned} \quad (\text{B1})$$

where

$$\begin{aligned} R_k(j, l) &= \sum_{m=0}^{\infty} E \left( k - \sum_{q=1}^{N-1} qm_q \right) \\ &\quad \times \prod_{q=0}^{N-1} G_{j_q}(m_q, -c_{qk}\lambda_N) G_{l_q}(m_q, -c_{qk}\lambda_N), \end{aligned} \quad (\text{B2})$$

and the  $G$  function has been defined in Eq. (7.4). Note that Eqs. (B1) and (B2) are exact, even if  $c_{qk}$  are obtained approximately. Because of the nearest-neighbor interaction, the matrix elements  $R_k(j, l)$  are given by

$$\begin{aligned} R_k(j, l) &= \hbar\omega_0 \epsilon_0 \delta_{j_0, l_0} \delta_{j_1, l_1} \cdots \delta_{j_{N-1}, l_{N-1}} \\ &\quad - \frac{1}{2} \hbar\omega_0 B \left\{ e^{i2\pi k/N} \prod_{q=0}^{N-1} \right. \\ &\quad \times \left[ \sum_{m_q=0}^{\infty} e^{-i2\pi q m_q/N} G_{j_q}(m_q, -c_{qk}\lambda_N) \right. \\ &\quad \left. \left. \times G_{l_q}(m_q, -c_{qk}\lambda_N) \right] + \text{c.c.} \right\}. \end{aligned} \quad (\text{B3})$$

Using the relation

$$\begin{aligned} \sum_{m=0}^{\infty} r^m \frac{u^m}{m!} \frac{m!}{u^l(m-l)!} \frac{m!}{u^n(m-n)!} \\ = \frac{r^l}{u^l} \frac{d^n}{du^n} (u^l e^{ru}), \quad l \geq n, \end{aligned} \quad (\text{B4})$$

we can perform the sum over  $m_q$  analytically and obtain the diagonal matrix elements of  $R_k$ ,

$$\begin{aligned} R_k(j, j) &= \hbar\omega_0 \epsilon_0 - \frac{1}{2} \hbar\omega_0 B \\ &\quad \times \left[ e^{i2\pi k/N} \prod_{q=1}^{N-1} Z(e^{-i2\pi q/N}, j_q, c_{qk}^2 S_N) + \text{c.c.} \right], \end{aligned} \quad (\text{B5})$$

where

$$\begin{aligned} Z(r, j, u) &= \frac{e^{u(r-1)}}{j!} \sum_{l, n=0}^j (-1)^{l+n} \binom{j}{l} \\ &\quad \times \binom{j}{n} \sum_{i=0}^{\min(l, n)} i! \binom{l}{i} \binom{n}{i} r^{l+n-i} u^{j-i}. \end{aligned} \quad (\text{B6})$$

Equations (B5) and (B6) are Eqs. (7.6) and (7.7), respectively.

The function  $Z$  has the properties

$$Z(r, j, 0) = r^j, \quad (\text{B7a})$$

$$Z(1, j, u) = \sum_{m=0}^{\infty} [G_j(m, -\sqrt{u})]^2 = 1, \quad (\text{B7b})$$

$$Z^*(r, j, u) = Z(r^*, j, u), \quad \text{for real } u. \quad (\text{B7c})$$

Equation (B7b) is a special case of relation (A6) and has been used in obtaining Eq. (B5) from Eq. (B3). Written out explicitly, the first three  $Z(r, j, u)$ 's are

$$Z(r, 0, u) = e^{u(r-1)}, \quad (\text{B8a})$$

$$Z(r, 1, u) = e^{u(r-1)} [u + r(ru + 1) - 2ru], \quad (\text{B8b})$$

$$\begin{aligned} Z(r, 2, u) &= e^{u(r-1)} \left[ \frac{1}{2} u^2 + 2ru(ru + 1) \right. \\ &\quad \left. + r^2 \left( \frac{1}{2} r^2 u^2 + 2ru + 1 \right) \right. \\ &\quad \left. - 2ru^2 + r^2 u^2 - 2r^2 u(ru + 2) \right], \end{aligned} \quad (\text{B8c})$$

which indeed satisfy Eqs. (B7).

<sup>1</sup>L. D. Landau, Phys. Z. Sowjetunion **3**, 664 (1933); S. I. Pekar, Zh. Eksp. Teor. Fiz. **16**, 335 (1946); L. D. Landau and S. I. Pekar, *ibid.* **18**, 419 (1948).

<sup>2</sup>H. Fröhlich, Proc. R. Soc. London, Ser. A **215**, 291 (1952); Adv. Phys. **3**, 325 (1954).

<sup>3</sup>T. Holstein, Ann. Phys. (N.Y.) **8**, 325 (1959).

<sup>4</sup>T. Holstein, Ann. Phys. (N.Y.) **8**, 343 (1959).

- <sup>5</sup>Y. Toyozawa, *Prog. Theor. Phys.* **26**, 29 (1961).
- <sup>6</sup>T. D. Lee, F. Low, and D. Pines, *Phys. Rev.* **90**, 297 (1953).
- <sup>7</sup>E. I. Rashba, in *Excitons*, edited by E. I. Rashba and M. D. Sturge (North-Holland, Amsterdam, 1982).
- <sup>8</sup>V. M. Kenkre and P. Reineker, *Exciton Dynamics in Molecular Crystals and Aggregates*, Springer Tracts in Modern Physics Vol. 94, edited by G. Höhler (Springer, Berlin, 1982).
- <sup>9</sup>A. S. Davydov, *Solitons in Molecular Systems* (Reidel, Boston, 1985).
- <sup>10</sup>M. Ueta, H. Kanzaki, K. Kobayashi, Y. Toyozawa, and E. Hanamura, *Exciton Processes in Solids*, Springer Series in Solid-State Sciences Vol. 60 (Springer, Berlin, 1986).
- <sup>11</sup>A. J. Heeger, S. Kivelson, J. R. Schrieffer, and W.-P. Su, *Rev. Mod. Phys.* **60**, 781 (1988).
- <sup>12</sup>A. A. Gogolin, *Phys. Rep.* **157**, 348 (1988).
- <sup>13</sup>A. J. Fisher, W. Hayes, and D. S. Wallace, *J. Phys. Condens. Matter.* **1**, 5567 (1989).
- <sup>14</sup>R. P. Feynman, *Phys. Rev.* **97**, 660 (1955).
- <sup>15</sup>R. E. Merrifield, *J. Chem. Phys.* **40**, 445 (1964).
- <sup>16</sup>H. B. Shore and L. M. Sander, *Phys. Rev. B* **7**, 4537 (1973).
- <sup>17</sup>H. Sumi, *J. Phys. Soc. Jpn.* **36**, 770 (1974).
- <sup>18</sup>G. B. Norris and G. Whitfield, *Phys. Rev. B* **21**, 3558 (1980).
- <sup>19</sup>Y. Toyozawa, in *Organic Molecular Aggregates*, Springer Series in Solid-State Sciences Vol. 49, edited by P. Reineker, H. Haken, and H. C. Wolf (Springer, Berlin, 1983), p. 90.
- <sup>20</sup>S. Fischer, in *Organic Molecular Aggregates*, Springer Series in Solid-State Sciences Vol. 49, edited by P. Reineker, H. Haken, and H. C. Wolf (Springer, Berlin, 1983), p. 107.
- <sup>21</sup>P. O. Scherer and S. F. Fischer, *Chem. Phys.* **86**, 269 (1984); E. W. Knapp, P. O. J. Scherer, and S. F. Fischer, *Chem. Phys. Lett.* **111**, 481 (1984).
- <sup>22</sup>F. M. Peeters, Wu Xiaoguang, and J. T. Devreese, *Phys. Rev. B* **33**, 3926 (1986).
- <sup>23</sup>D. Emin, *Phys. Today* **35**, No. 1, 34 (1982), and references therein.
- <sup>24</sup>D. W. Brown, K. Lindenberg, and B. J. West, *Phys. Rev. A* **33**, 4104 (1986); **35**, 6169 (1987); *Phys. Rev. Lett.* **57**, 2341 (1986); *J. Chem. Phys.* **87**, 6700 (1987); D. W. Brown, B. J. West, and K. Lindenberg, *Phys. Rev. A* **33**, 4110 (1986); X. Wang, D. W. Brown, K. Lindenberg, and B. J. West, *ibid.* **37**, 3557 (1988).
- <sup>25</sup>Z. Ivic and D. W. Brown, *Phys. Rev. Lett.* **63**, 426 (1989); D. W. Brown and Z. Ivic, *Phys. Rev. B* **40**, 9876 (1989).
- <sup>26</sup>P. S. Lomdahl and W. C. Kerr, *Phys. Rev. Lett.* **55**, 1235 (1985).
- <sup>27</sup>W. C. Kerr and P. S. Lomdahl, *Phys. Rev. B* **35**, 3629 (1987).
- <sup>28</sup>Q. Zhang, V. Romero-Rochin, and R. Silbey, *Phys. Rev. A* **38**, 6409 (1988).
- <sup>29</sup>M. J. Skrinjar, D. V. Kapor, and S. D. Stojanovic, *Phys. Rev. A* **38**, 6402 (1988).
- <sup>30</sup>W. Rhodes and A. Nicholls, *Phys. Rev. Lett.* **64**, 1174 (1990).
- <sup>31</sup>L. A. Turkevich and T. D. Holstein, *Phys. Rev. B* **35**, 7474 (1987); T. D. Holstein and L. A. Turkevich, *ibid.* **38**, 1901, 1923 (1987).
- <sup>32</sup>H. Sumi, *J. Phys. Soc. Jpn.* **38**, 825 (1975).
- <sup>33</sup>S. Abe, *J. Phys. Soc. Jpn.* **57**, 4029, 4036 (1988).
- <sup>34</sup>R. Friesner and R. Silbey, *J. Chem. Phys.* **74**, 1166 (1981).
- <sup>35</sup>R. Friesner and R. Silbey, *J. Chem. Phys.* **74**, 3925, 5630 (1981).
- <sup>36</sup>R. E. Lagos and R. A. Friesner, *J. Chem. Phys.* **81**, 5899 (1984); Y. Won, R. Lagos, and R. Friesner, *ibid.* **84**, 6567 (1986).
- <sup>37</sup>P. O. J. Scherer, E. W. Knapp, and S. F. Fischer, *Chem. Phys. Lett.* **106**, 191 (1984).
- <sup>38</sup>F. C. Spano, J. R. Kuklinski, and S. Mukamel [*Phys. Rev. Lett.* **65**, 211 (1990)] have numerically calculated the size (and the temperature) effects on the superradiative decay rate of the cyclic molecular aggregates by using a perturbation method in the region of exciton bandwidth being much larger than the relaxation energy ( $2B \gg S$ ).
- <sup>39</sup>Due to the periodicity  $N$  of the exciton states  $|k\rangle$ 's, the subspace with the total (exciton + phonon) momentum  $k + lN$  ( $l$  is an arbitrary integer) is the same subspace with the total (exciton + phonon) momentum  $k$ .
- <sup>40</sup>E. Daltorozzo, G. Scheibe, K. Gschwind, and F. Haimerl, *Phot. Sci. Eng.* **18**, 441 (1974).
- <sup>41</sup>P. Scherer, B. Kopainsky, and W. Kaiser, *Opt. Commun.* **39**, 375 (1981); B. Kopainsky, J. K. Hallermeier, and W. Kaiser, *Chem. Phys. Lett.* **83**, 498 (1981); **87**, 7 (1982).
- <sup>42</sup>S. DeBoer, K. J. Vink, and D. A. Wiersma, *Chem. Phys. Lett.* **137**, 99 (1987); S. DeBoer and D. A. Wiersma, *ibid.* **165**, 45 (1990).
- <sup>43</sup>For a review on the Green's function, including the (static) coherent potential approximation, see E. N. Economou, *Green's Function in Quantum Physics*, Springer Series in Solid-State Sciences Vol. 7 (Springer, Berlin, 1983).
- <sup>44</sup>B. Velicky, *Phys. Rev.* **184**, 614 (1969).
- <sup>45</sup>M. Aihara and A. Kotani, *Solid State Commun.* **46**, 751 (1983).
- <sup>46</sup>S. Mukamel, *Phys. Rep.* **93**, 1 (1982).
- <sup>47</sup>B. R. Mollow, *Phys. Rev.* **188**, 1969 (1969).
- <sup>48</sup>B. R. Mollow, *Phys. Rev. A* **5**, 2217 (1972).